AD_____

Award Number: DAMD17-00-1-0548

TITLE: Magnetic Resonance Spectroscopy Imaging and Functional Magnetic Resonance Imaging of Neurofibromatosis Type 1: In Vivo Pathophysiology, Brain-Behavior Relationships, and Reading Disabilities

PRINCIPAL INVESTIGATOR: Laurie E. Cutting, Ph.D.
Peter Barker, Ph.D., Alena Horska, Ph.D.,
Walter Kaufman, M.D., Christine W. Koth,
Stewart Mostofsky, M.D.

CONTRACTING ORGANIZATION: Kennedy Krieger Institute
Baltimore, Maryland 21205

REPORT DATE: October 2001

TYPE OF REPORT: Annual

PREPARED FOR: U.S. Army Medical Research and Materiel Command
Fort Detrick, Maryland 21702-5012

REPORT DOCUMENTATION PAGE

Form Approved
OMB No. 074-0188

1. AGENCY USE ONLY (Leave blank)	2. REPORT DATE	3. REPORT TYPE AND DATES COVERED
	October 2001	Annual (01 Oct 00 - 30 Sep 01)

4. TITLE AND SUBTITLE
Magnetic Resonance Spectroscopy Imaging and Functional Magnetic Resonance Imaging of Neurofibromatosis Type 1: In Vivo Pathophysiology, Brain-Behavior Relationships, and Reading Disabilities

5. FUNDING NUMBERS
DAMD17-00-1-0548

6. AUTHOR(S)
Laurie E. Cutting, Ph.D., Peter Barker, Ph.D., Alena Horska, Ph.D., Walter Kaufman, M.D., Christine W. Koth, Stewart Mostofsky, M.D.

7. PERFORMING ORGANIZATION NAME(S) AND ADDRESS(ES)
Kennedy Krieger Institute
Baltimore, Maryland 21205

E-Mail: cutting@kennedykrieger.org

8. PERFORMING ORGANIZATION REPORT NUMBER

9. SPONSORING / MONITORING AGENCY NAME(S) AND ADDRESS(ES)
U.S. Army Medical Research and Materiel Command
Fort Detrick, Maryland 21702-5012

10. SPONSORING / MONITORING AGENCY REPORT NUMBER

11. SUPPLEMENTARY NOTES

12a. DISTRIBUTION / AVAILABILITY STATEMENT
Approved for Public Release; Distribution Unlimited

12b. DISTRIBUTION CODE

13. ABSTRACT ***(Maximum 200 Words)***

The purpose of this research is oriented towards understanding the reading, language, and articulation deficits associated with Neurofibromatosis Type 1 (NF-1) and relating these deficits to the underlying pathophysiology of NF-1 as revealed by Magnetic Resonance Spectroscopy Imaging (MRSI). A second goal is to determine how differences in activation, as measured by functional Magnetic Resonance Imaging (fMRI), are linked to the cognitive/academic impairments associated with NF-1. A third goal is to further understand how T-2 weighted hyperintensities on Magnetic Resonance Imaging (MRI) scans are related to cognitive/academic impairments associated with NF-1. Each aim addresses the research in terms of pathophysiology and how cognitive/academic functioning of children with NF-1 compares to control groups when examined in both genetic (i.e., sibling) as well as general population (both reading disabled and non-reading disabled) contexts. We hypothesize that abnormalities of NAA, Choline, or their ratios, will exist in the thalamus and will correlate with language, reading, and articulation deficits in NF-1, defined by "lowering" of the cognitive scores of each child with NF-1 relative to his/her unaffected sibling. For the second goal, we hypothesize that children with NF-1 will activate their brains similarly to reading disabled children during fMRI tasks. For the third goal, we hypothesize that reading, language, and articulation deficits will correlate with the number of brain locations with T2-weighted hyperintensities. Thus, neuroimaging permits the pursuit of furthering our understanding of how the NF-1 gene affects the brain in terms of basic neurobiologic factors (ultrastructural, physiological, and localization) as well as their impacts on cognition (reading, language, and articulation) in NF-1.

14. SUBJECT TERMS
Learning Disability Diagnosis, Neurofibromatosis Type 1, functional Magnetic Resonance Imaging, anatomical Magnetic Resonance Imaging, Magnetic Resonance Spectroscopy Imaging, Reading, and Speech/Language Disorder

15. NUMBER OF PAGES
74

16. PRICE CODE

17. SECURITY CLASSIFICATION OF REPORT	18. SECURITY CLASSIFICATION OF THIS PAGE	19. SECURITY CLASSIFICATION OF ABSTRACT	20. LIMITATION OF ABSTRACT
Unclassified	Unclassified	Unclassified	Unlimited

TABLE OF CONTENTS

INTRODUCTION

The purpose of this research is primarily oriented towards understanding and documenting the reading, language, and articulation deficits associated with Neurofibromatosis Type 1 (NF-1) and relating these deficits to the underlying pathophysiology of NF-1 as revealed by Magnetic Resonance Spectroscopy Imaging(MRSI). A second goal is to determine how differences in activation, as measured by functional Magnetic Resonance Imaging (fMRI), are linked to the cognitive and academic impairments associated with NF-1. A third goal is to further understand how the brain's visible abnormalities, T-2 weighted hyperintensities on Magnetic Resonance Imaging (MRI) scans, are related to the reading, language, and articulation deficits in NF-1. Each of the specific aims of the research addresses components of the research in terms of pathophysiology and how cognitive/academic functioning of children with NF-1 compares to control groups when examined in both genetic (i.e., sibling) as well as general population (both reading disabled and non-reading disabled) contexts. Based upon previous research findings, we hypothesize that abnormalities of NAA, Choline, or their ratios, will exist in the thalamus; further, that thalamic abnormalities will correlate with language, reading, and articulation deficits in NF-1, as defined by the "lowering" of the cognitive score of each child with NF-1 relative to that of his/her unaffected sibling. In terms of the second goal of this research, we hypothesize that children with NF-1 will activate their brains similarly to reading disabled children during fMRI tasks. In terms of the third goal of this research, we hypothesize that reading, language, and articulation deficits will (as reported for IQ) correlate with the number of brain locations in which T2-weighted hyperintensities are seen. Thus, the use of MRI, MRSI, and fMRI methodology in this research permits the pursuit of further understanding the basic neurobiologic factors (ultrastructural, physiological, and localization) as well as their impacts on cognition (reading, language, and articulation) in NF-1, thus furthering our understanding of how the NF-1 gene affects the brain.

BODY

Research Accomplishments Associated With Each Task: Tasks 1 and 2, which were targeted for years one and two of the grant, have been addressed during the first year of the grant. Task 1 dealt with subject recruitment and data collection (targeted for months 1-26), and included the goals of recruiting patients for participation, screening patients for eligibility, and conducting onsite neuropsychological evaluations and MRSI/fMRI procedures. Task 2 dealt with analyzing data (months 3-26). Tasks 3 and 4, data entry and statistical analysis of MRI and neuropsychological data (months 20-32) and results/manuscript preparation (months 20-36) were targeted for this coming year as well as the third year of the grant, although we have entered our data and done some statistical analyses already.

Number of Patients Seen: We have seen 18 patients altogether, nine with NF-1, eight without NF-1, and one child with a reading disability (RD); three of the nine patients with NF-1 were sibling pairs. One patient with NF-1 did not meet criteria for being included in the study because she had an IQ lower than 80; however, this did not present a problem because she participated fully in the testing and the parents received appropriate feedback (i.e., she will not be included in data analyses). Below is a chart of the participants:

	1ST YEAR	**GOAL OVER 3YRS**	**% OF TOTAL**
NF-1	6	20	30%
NF-1 W/SIBLING	3	10	33%
NF-1 SIBLING (NON AFFECTED)	3	10	33%
CONTROLS	5	20	25%
READING DISABILITIES	1	30	3%
TOTAL NUMBER SEEN:	**18**	**95**	**19%**

Preliminary Findings/Progress: Findings from the neuropsychological data between children with NF-1 and non-affected children are presented below; we do not yet have enough data from the MRI components of the grant to present findings. Data from the 3 MRSI scans we have collected are in the process of being analyzed by Dr. Barker's group. For the fMRI component of the grant, we are developing the paradigms and piloting the fMRI tasks.

Preliminary analyses comparing children with and without NF-1 (we excluded the 1 subject with RD from analyses) on the language and reading measures suggest that within these areas, some functions are impaired for children with NF-1, while others are not. Analyses of Variance (ANOVAs) conducted using Performance IQ as a covariate suggest that children with NF-1 have weaknesses in receptive and expressive language, phonological awareness, and reading accuracy (decoding). On the other hand, results suggested that immediate memory, ability to make inferences, reading comprehension, and rate of retrieval appear to be relatively spared. If these findings prove to be true, intervention for the associated learning disabilities in children with NF-1 will be able to be tailored to this pattern of strengths and weaknesses (e.g., strong inferential abilities may help remediate language disabilities). The preliminary results are listed in Table 1:

Table 1

TEST / Subtest	P-value* $
Clinical Evaluation of Language Fundamentals – 3 (CELF-3); Receptive Language	**.01**
CELF-3; Expressive Language	**.001**
Test of Language Competence (TLC); Ambiguous Sentences	**.04**
TLC; Figurative Language	**.03**
TLC; Inferences	**n.s.**
Gray Oral Reading Test – 3 (GORT-3); Reading Accuracy	**.05**
GORT-3; Reading Rate	**.03**
GORT-3 Comprehension	**n.s.**
Wide Range Test of Memory and Learning (WRAML); Immediate Recall	**n.s.**
Weschler Individual Achievement Test (WIAT); Basic Reading	**.002**
WIAT; Reading Comprehension	**n.s.**
WIAT; Listening Comprehension	**n.s.**
Comprehensive Test of Phonological Processing (CTOPP); Phonological Awareness	**.01**
CTOPP; Phonological Memory	**n.s.**
CTOPP; Rapid Automatized Naming	**n.s.**

*all significant values showed that children with NF-1's performance was lower than children without NF-1

$Note that Performance IQ was used as a covariate

Problems in Accomplishing Tasks: We have had some significant "external" impediments that have not allowed us to recruit and evaluate subjects for a total six months of this first year of the grant (50% of the first year). This was due to two reasons. The first was, understandably, the need for final approval from the US Army Medical Research and Material Command Human Subjects board, part of which involved establishing liability agreements between the Army and Johns Hopkins Medical Institutions, which held us up from starting to see subjects until February. The second was from the shut down of all research at Johns Hopkins Medical Institutions mandated by the Office for Human Research Protections (OHRP), which happened in July. Due to this "shut down" of all research, Johns Hopkins Medical Institutions had to re-evaluate all protocols, which resulted in our not being able to see subjects from mid-July through mid-September. Nonetheless, despite these two substantial setbacks, we have managed to see adequate numbers of subjects and have had significant success in recruiting subjects (unfortunately 6 subjects were scheduled to come in for testing in July and August and had to be cancelled, but are currently being re-scheduled).

Recommended Changes: So far, we have not encountered any issues that suggest that we should consider changing our goals/procedures of the grant in any manner. We do not anticipate any obstacles in our research in the second year, so we anticipate, based on our first year of success, a highly productive coming year.

KEY RESEARCH ACCOMPLISHMENTS

- Have identified and established connections with many recruiting sources
- Have seen 18 subjects
  - 3 sibling pairs
- Have entered all neuropsychological data and begun preliminary statistical analyses
- Have collected MRSI data for 3 (out of a goal of 10) NF-1s from sibling pairs
- Developing fMRI paradigms

REPORTABLE OUTCOMES

There are no reportable outcomes as of yet which have resulted directly from this grant. However, while not directly resulting from the data collected from this grant, this grant has helped support our overall program of research on NF-1 at the Kennedy Krieger Institute. This includes two publications. One publication, currently under revision in *Neurology*, provides detailed analyses of cortical gray and white matter volumes in males with NF-1; lobar (frontal, occipital, parietal, and temporal lobes) and lobar subdivisions (e.g., prefrontal lobe) areas were measured. Findings indicated that NF-1 was associated with larger cerebral gray and white matter volumes with larger frontal and parietal white matter volumes (including somatosensory white matter volumes) than controls. Another publication (submitted to the *American Journal of Medical Genetics*) examined the longitudinal evolution of T2-weighted hyperintensities (UBOs). Findings showed that the total number of UBO-occupied locations evolved in a non-linear manner, with a decrease between approximately ages 7-12 years, followed by a progressive increase in adolescence. The same pattern was also found for UBO number and/or volume for all regions, with the exception of cerebellar hemispheres.

We have applied for funding from the National Institutes of Health (NIH; R01 HD 41054-01A1). The NIH grant that has been applied for relates to our understanding of idiopathic reading and language disorders, which is relevant to treating the reading and language disorders prevalent in NF-1.

CONCLUSIONS

Despite our inability to recruit and evaluate subjects for six months of the first year of the grant due to 1) final Human Subjects approval from US Army Medical Research and Material Command and 2) Johns Hopkins Medical Institutions re-evaluation of protocols, we have seen adequate numbers of subjects. We have had a constant flow of subjects when we have been able to be "in operation", and have begun to address many of the goals of the grant. We do not anticipate any further other halts in our research this coming fiscal year and project that we will able to see approximately one subject per

week. Preliminary findings suggest that children with NF-1 have both strengths and weaknesses within the reading and language domain; weaknesses were found in receptive and expressive language, phonological awareness, and reading accuracy (decoding), with relative strengths in immediate memory, ability to make inferences, reading comprehension, and rate of retrieval. If these findings prove to be true with a greater number of subjects, intervention for the associated learning disabilities in children with NF-1 will be able to be tailored to this pattern of strengths and weaknesses (e.g., strong inferential abilities may help remediate language disabilities). This grant has also helped support our overall program of research on NF-1 at the Kennedy Krieger Institute. This includes two publications (one under revision in *Neurology* and another submitted to *American Journal of Medical Genetics*).

REFERENCES

None.

APPENDICES

Cutting, L.E., Cooper, K.L., Koth, C.W., Mostofsky, S.H., Kates, W.R., Denckla, M.B., and Kaufmann, W.E. (under revision). Gray and White Matter Volumes in Children with Neurofibromatosis Type 1 with and without ADHD. *Neurology*.

Kraut, M.A., Gerring, J.P., Cooper, K.L, Thompson, R.E., Denckla, M.B., Kaufmann, W.E. (submitted). Longitudinal Evolution of T2-Weighted Hyperintensities in Children with Neurofibromatosis Type 1. *American Journal of Medical Genetics.*

MS#200100147

Gray and White Matter Volumes in Children with Neurofibromatosis Type 1 with and without ADHD

L.E. Cutting, PhD, K.L. Cooper, BA, C.W. Koth, MS,

S.H. Mostofsky, MD, W.R. Kates, PhD, M.B. Denckla, MD, and W.E. Kaufmann, MD

From the aMRI Analysis Laboratory, Kennedy Krieger Institute, and the Departments of Neurology, Psychiatry, Pediatrics, Pathology, and Radiology, Johns Hopkins University School of Medicine, Baltimore, Maryland

Acknowledgments: The authors thank Michael Kraut, MD, for neuroradiologic assistance and Diane Lanham, MA, for help in data collection and analysis. This work was supported by grants P50 NS 35359 and P30 HD 24061 from the National Institutes of Health and a grant from the Department of Defense, DAMD 17-00-1-0548.

Running Head: Cerebral Gray/White, neurofibromatosis-1 and ADHD

Word Count: 4,809
Character Count: 94

Address correspondence and reprint requests:

Walter E. Kaufmann, M.D.
Department of Developmental Cognitive Neurology
The Kennedy Krieger Institute
707 N. Broadway, Room 522
Baltimore, Maryland 21205
Phone: 410-502-9012
Fax: 410-502-9364
Email: wekaufma@jhmi.edu

Article Abstract

Background: Megalencephaly is a frequent CNS manifestation in neurofibromatosis type 1 (NF1); however, its regional pattern, tissue composition, modification by ADHD, and relationship with unidentified bright objects (UBOs) remain controversial.

Methods: Eighteen males with NF1, seven of whom had ADHD (NF1+ADHD), were compared with 18 age-, gender-matched controls in terms of MRI-, Talairach-based brain, cerebral, and lobar gray and white matter volumes. Twelve subjects with NF1 had UBOs in the centrencephalic region, while 6 had no UBO or exclusively infratentorial lesions.

Results: NF1 males without ADHD (NF1-pure) had the largest total cerebral, gray, and white matter volumes with larger parietal, namely somatosensory, white matter volumes than controls, particularly if UBOs were present in the basal ganglia. All subjects with NF1 (including NF1+ADHD) had larger total and frontal white matter volumes than controls. Smaller frontal, namely right prefrontal, gray matter volumes were found in NF1+ADHD when compared with NF1-pure.

Conclusions: The increase in frontal and parietal white matter volumes in males with NF1, including its preferential centrencephalic distribution supports the hypothesis that NF1's white matter pathology encompasses but is not limited to visible UBOs. Males with NF1+ADHD as compared with NF1-pure, showed frontal reductions, which in general terms are consistent with those found in idiopathic ADHD.

Neurofibromatosis Type 1 (NF1) is the most common autosomal dominant genetic disorder affecting the central nervous system, with a prevalence of approximately 1:3500 in the population .[1,2] Brain manifestations include tumors (most often optic gliomas), megalencephaly, and corpus callosum anomalies.[3] On magnetic resonance imaging (MRI) scans, many children show T2-weighted hyperintensities/unidentified bright objects (UBOs).[3] These lesions are located in many regions, including brainstem, cerebellum, thalamus, and basal ganglia, with a predominance in the latter.[3] Aside from these physical features, cognitive and behavioral impairments are frequently associated with NF1, in particular learning disabilities (25-61 %[1,4,5] vs. 7-10% in the general population).[6]

Most of the MRI research in patients with NF1 has focused on the presence and location of UBOs and how these may influence cognition.[4,7] Less has been reported about what MRI reveals about the megalencephaly, which underlies the macrocephaly observable in 50% of patients with NF1. Recent studies have confirmed that patients with NF1 have larger whole brain volumes on average than controls, with approximately half of patients with NF1 being megalencephalic.[8,9,10,11] Presence of megalencephaly has not been found to be associated with presence of UBOs, but it has been found to be associated with selective cognitive impairment[8] and other MRI signal abnormalities.[11] Differential gray and white matter contributions to megalencephaly have been examined by MRI morphometric studies. Two analyses found that white matter volumes were increased in patients with NF1 compared to controls,[10,11] while another recent study found that gray matter volumes were increased in patients with NF1.[9] Discordance between these studies[9,10,11] may be explained by differences

in MRI methodology and characteristics of the NF1 subjects (i.e. Attention Deficit Hyperactivity Disorder co-morbidity).

Attention Deficit Hyperactivity Disorder (ADHD) is present in clinical and research groups with NF1[12,13,14] with a higher prevalence than in the general population.[15] To date, only one other neuroimaging study has examined the relationship between NF1 and ADHD.[12] These authors found that total and rostral body and anterior midbody areas of the corpus callosum were significantly larger in NF1 groups (both with and without ADHD) as compared to controls, but the posterior midbody was significantly larger only in the NF1 group without ADHD.[12] The lack of enlargement of the posterior midbody in individuals with NF1 and ADHD suggests that the mechanisms underlying ADHD in NF1 have an opposite neurobiologic effect on callosal size compared with those operating in pure NF1. This reductive effect is consistent with the literature on idiopathic ADHD, which reports reductions affecting the whole cerebrum, as well as frontal regions, caudate, globus pallidus, and posterior inferior cerebellar vermis.[16-22]

Recent studies using different MR techniques provide evidence in support of a generalized cerebral white matter involvement in NF1. Using MR spectroscopy imaging (MRSI), we found, contrary to expectation, that in NF1 decreased N-acetylaspartate (NAA)/Choline (Cho) ratios were not specifically confined to areas with past or present UBOs, but instead were seen in other regions such as the thalamus.[23] Moreover, increases in Cho characterized younger subjects while older individuals showed reduced NAA.[23] A recent diffusion-weighted imaging investigation found increased water diffusion in multiple regions, which

was more severe in areas of UBOs.[24] The relationship between changes in tissue MR signal and megalencephaly is underscored by a recent study demonstrating a generalized increase in T1 signal that was more marked in megalencephalic subjects with NF1.[11] Based on these data and a previous neuropathologic study on NF1 demonstrating intramyelinic edema,[25] we hypothesize that in NF1 there is an early disruption in myelin that, despite attempts at repair, evolves to axonal injury in older subjects. UBOs would represent a salient feature of this process that would also result in cerebral white matter enlargement. In order to further characterize the cerebral enlargement in NF1, and to test our hypothesis, we extended our previous MRI study[8] to a regional characterization of cerebral volumes. Specifically, we sought to confirm that enlarged white matter is the main contributor to megalencephaly in children with NF1, that this cerebral increase is regionally related to UBOs, and that underlying ADHD in NF1 leads to a mitigation of megalencephaly.

Methods

Subjects. Subjects with NF1 were recruited as part of a larger research-center-based investigation of genetic and learning disabilities, "Neurodevelopmental Pathways to Learning Disabilities", at the Kennedy Krieger Institute in Baltimore, Maryland. Children affected with either familial or sporadic NF1 were diagnosed based on the National Institutes of Health consensus criteria.[1] Subjects were excluded if they had any intracranial pathology, including optic gliomas and other brain tumors, history of seizures, or any significant uncorrectable hearing or visual impairments. For a positive diagnosis of ADHD, subjects had to score positively on two or more of the following measures: the Attention Deficit Hyperactivity Scale from the Diagnostic Interview for Children – Revised - Parent Version

(DICA-R-P), with diagnosis based on positive endorsement of eight of the 14 items;[26,27] the Dupaul ADHD Rating Scale, with diagnosis based on a score of two or higher (on a 4-point Likert scale ranging from 0-3) for six out of nine items assessing inattention, and/or six out of nine items assessing hyperactivity/impulsivity;[28,29] the Attention Problem Index of the Child Behavior Checklist (CBCL),[30] with a score of at least 1.5 standard deviations above the mean (T- score $\geq$ 65); and the Hyperactivity Index on the Conners' Rating Scale – Revised – Parent Version,[31] with a score of at least 1.5 standard deviations above the mean (T- score $\geq$ 65). Control subjects included unaffected siblings from projects within the research center, as well as subjects recruited through offices of a local pediatrician. The pediatrician sent letters to parents of patients who, according to their medical record, did not have emotional problems or learning disabilities. Parents then contacted the Kennedy Krieger Institute if they were interested in participating in the study, were screened first by telephone, and then brought in for testing if they met criteria.

Each subject was screened for the presence of psychopathologies, including ADHD. Two NF1 subjects were administered only the DICA-R-P. IQ was in the normal range for all subjects as determined by the appropriate Wechsler Intelligence Scale[32,33,34] at time of testing. One adult control subject did not have IQ data available, but school records indicated normal aptitude, and one control subject was administered the Stanford-Binet Intelligence Scale.[35] One subject from NF1+ADHD group had a Full Scale IQ (FSIQ) of 78. One control subject had a previous diagnosis of bipolar disorder and another had a diagnosis of anxiety; both subjects had normal MRIs. All other control subjects were determined to be free of any psychopathologies.

With respect to race, two control subjects were African-American, one NF1-pure subject was Asian, and the remaining subjects were Caucasian of various ethnic origins. The prevalence rates of NF1 are comparable for males and females, but this study was confined to males in order to reduce the number of independent variables in the study, especially when the focus is on volumetrics. Moreover, the mitigation by ADHD of NF1-associated megalencephaly would be different if females with ADHD, whose total brain volume is generally not reduced,[22] were included.

The sample, ranging in age from 5.79 through 24.38 years, consisted of 18 males with NF1, (mean age 11.77 ± 3.83; mean FSIQ = 98.33 ± 14.62) and 18 age-matched male controls (mean age 11.99 ± 4.44; mean FSIQ = 121.41 ± 11.08). Seven of the eighteen males with NF1 were diagnosed with ADHD (NF1+ADHD mean age 10.87 ± 5.03; mean FSIQ = 90.86 ± 8.17). The remaining eleven of the eighteen males with NF1 had no other clinical diagnosis at the time of scan (NF1-pure mean age 12.34 ± 2.96; mean FSIQ = 103.09 ± 16.10). All of the NF1 subjects included in this study participated in a previous study on megalencephaly in NF1[8] and sixteen of the eighteen NF1 subjects in this study also participated in a study of the prevalence of ADHD among NF1 subjects and their unaffected siblings.[13]

The majority of participants with NF1 who were five through 14 years were individually age-matched within six months to controls; the rest were individually age-matched within a year to controls. Two 15 year-old NF1 males were age-matched within two years to controls, and

one 18 year-old male in the NF1 group was age-matched to a 24 year-old adult male control. The study was explained to all participants in language appropriate to their level of cognitive functioning. Each participant and parent signed assent and consent forms that met the institutional review board standards of the Johns Hopkins Medical Institutions and the Joint Committee on Clinical Investigation approved the protocol.

MRI technique. All subjects were evaluated with routine brain MRI scans (T1-weighted and T2-weighted sequences) and 3-D volumetric radiofrequency spoiled gradient (SPGR) scans. All scans were performed on a 1.5 T General Electric Signa Scanner (Milwaukee, Wisconsin) using the standard GE quadrature head coil. The MR protocol consisted of the following series: sagittal T1 and axial spin-density/T2-weighted brain MRI, followed by SPGR with the following scan parameters: TR=35-45, TE= 5-7, flip angle=45, NEX=1, matrix size=256x128, field of view=20-24. Each SPGR series was partitioned into 124, 1.5 mm contiguous slices. Five sagittal SPGR scans (two from the control group, three from the NF group), one axial SPGR (from the NF group), and 30 coronal SPGR scans (16 from the control group, seven from the NF-pure group, and seven from the NF+ADHD group) were used to obtain volumetric data for each subject. In a previous study we determined that no significant differences exist between the volumes obtained from coronal, sagittal, and axial scans.[8]

Routine spin-density/T2 MRI scans showed hyperintensities (UBOs) in 13 NF1 subjects. Eleven subjects had one or more UBO(s) in the basal ganglia and ten of those eleven also had infratentorial lesions. One subject had UBOs in the thalamus only, while another had only

cerebellar UBOs. NF1 subjects with UBOs in the basal ganglia or the thalamus were labeled as centrencephalic UBO positive (n=12) and all other NF1 subjects were labeled as centrencephalic UBO negative (n=6). Since the volumetric analyses are focused on cerebral changes, we have circumscribed our UBO analyses to this cerebral location (i.e., centrencephalic).

The raw, GE-Signa formatted image data were transferred to Apple Macintosh Power PC workstations via network connections. The SPGR image data was imported into the program *BrainImage*[36] for visualization, processing, and quantitation.[37] The importation process creates a 124-slice image stack composed of spatially registered, 8-bit images that have been processed to minimize signal artifacts related to RF field inhomogeneity. In order to prepare the stacks for measurement, non-brain material (e.g. skull, musculature, and vasculature) is removed from these image stacks using a semi-automated edge detection routine that involves region growing as well as stepwise morphological operations.[37] These "skull stripped" images are re-sliced so that the interpolated slice thickness (z-dimension) is the same as the x and y pixel dimensions thereby converting the image stacks into cubic voxel data sets. The cubic voxel data sets are opened into the multiplanar visualization module of *BrainImage*[36] so that three orthogonal representations of the data can be viewed simultaneously.

Isolated brain tissue was segmented into gray, white, and CSF compartments by a fuzzy segmentation protocol that uses an algorithm to assign voxels to one or more tissue categories based on intensity values and tissue boundaries.[38] The segmentation method used

was determined reliable for all gray matter, white matter, and CSF volumes.[38] The brain tissue was subdivided into cerebral lobes, subcortical, brainstem and cerebellar regions according to a revised Talairach stereotaxic grid[39] specific for measurement in pediatric study groups.[40,41,42] This approach has been shown to yield high levels of sensitivity and specificity for all lobar brain regions.[42] Due to their smaller size, the validity of the brainstem, cerebellar, and subcortical region measurements is lower, therefore, only cerebral and lobar volumes were included in the analyses. Based on our hypothesis postulating that fiber bundles originating in frontal and parietal regions are predominantly affected in NF1, particularly in those individuals with basal ganglia and thalamic UBOs, the frontal and parietal lobes were subdivided into functional units to further localize the volumetric differences between the groups. The frontal lobe was subdivided into the following regions: prefrontal, premotor, motor, deep frontal white matter, and anterior cingulate. The parietal lobe was subdivided into the following regions: somatosensory, dorsolateral parietal, inferior parietal, deep parietal white matter, and the posterior cingulate that includes a portion of the corpus callosum. A research assistant who was blind to the diagnosis of each subject carried out all measurements.

Statistical Analyses. Univariate (ANCOVAs) and multivariate (MANCOVAs) analyses were used to compare groups. Significance levels were set at an alpha level of .05. To control for Type I error, post-hoc tests were conducted only for those multivariate and univariate tests that revealed significance. Considering the dynamic nature of volumetric changes throughout childhood,[43,44,45] for all analyses, age was used as a covariate. Based on our previous study[8] demonstrating significantly larger total cerebral volumes in a large proportion of NF1

subjects, for lobar analyses the latter variable as well as age were used as covariates. As there were no significant correlations with IQ for cerebral volumes, we did not use IQ as a covariate (see Results section). Before beginning analyses with volumetric data, log transformations were performed to normalize the data. In addition, Games-Howell post-hoc tests, which do not assume equal Ns, cell normality, and can be used for Ns as small as 6,[46] were used for all post-hoc analyses. The sequence of analyses was decided *a priori* and was:

1. Total Cerebral Volume (TCV), comparing NF1-pure, NF1+ADHD, and controls.
2. Total white (TWCV) and gray (TGCV) cerebral volumes, as in step 1.
3. Any significant difference in total cerebral volume derived from step 2 (i.e., gray or white matter) to be further analyzed with regard to lobar divisions.
4. Any significant difference in frontal or parietal lobar volume derived from step 3 (i.e., gray or white matter) to be further analyzed with regard to frontal or parietal lobar subdivisions.
5. Cerebral, lobar, and sublobar white matter volumes to be compared between those in the NF1 groups (i.e., regardless of ADHD status) with and without UBOs in the centrencephalic region.

Results

Preliminary analyses. Previous behavioral studies have shown a slight decrease in FSIQ in subjects with NF1,[3,4] particularly those with ADHD co-morbidity,[13] and our preliminary analyses revealed significant differences among the three groups in FSIQ. The mean FSIQ of the NF1-pure and NF1+ADHD groups were significantly lower than that of the control group. The mean FSIQ of the NF1+ADHD group was lower although not significantly than

that of the NF1-pure group. There were no significant correlations with age or FSIQ for TCV, TGCV, or TWCV. There were no significant differences in age; however, given the large age range and the known brain developmental changes across this age range, especially with regard to white matter,[43-45] we covaried for age in our analyses.

We also examined the influence of age on TCV, TGCV, and TWCV by using age as a factor rather than covariate, in our analyses. On the bases of neuroimaging morphometric data, demonstrating growth cerebral peaks at about 12 years,[45] we divided the subjects into four groups: NF1 less than twelve years of age, NF1 equal to or greater than twelve years of age, controls less than twelve years of age, and controls equal to or greater than twelve years of age. The NF1 groups included both NF1-pure and NF1+ADHD subjects. Analyses were conducted between the groups for both TGCV and TWCV. Results of these analyses revealed that there were significant differences in TWCV between the groups split at age 12 (figure 1). However, the group by age interaction was not significant, indicating that increase in brain volumes occurs in a similar manner between NF1 and control groups (figure 1).

Insert Figure 1 about here

Main Analyses. Table 1 summarizes measurements and analyses of TCV, TGCV, TWCV, and lobar volumes. The ANCOVA for TCV revealed that the TCV of the NF1-pure group was 13% larger than that of NF1+ADHD and 15.6% larger than the control group $F(1, 32) =$

8.315, $p = .0012$. The TCV of NF1+ADHD group was 2.6% larger than that of the control group. The MANCOVA for TGCV and TWCV was significant; univariate and post-hoc analyses revealed that the TGCV of the NF1-pure group were larger than that of both the NF+ADHD and control groups $F(1, 32) = 6.386$, $p = .0046$, and the TWCV of the NF1-pure and NF1+ADHD groups were larger than that of the control group $F(1, 32) = 10.794$, $p = .0003$.

The MANCOVA for white matter lobar analyses was significant; univariate and post-hoc tests revealed that the parietal white matter ($F(1, 31) = 5.183$, $p = .0114$) volumes of the NF1-pure group were *larger* than those of the control group, and frontal white matter volumes of both the NF1-pure and NF1+ADHD groups were *larger* than those of the control group $F(1, 31) = 5.283$, $p = .0106$. The MANCOVA for gray matter lobar analyses was significant; univariate and post-hoc tests revealed that the frontal gray matter volumes of the NF1+ADHD group were significantly *smaller* than the NF1-pure group, $F(1, 31) = 8.422$, $p = .0012$.

Insert Table 1

Table 2 summarizes measurements and analyses of frontal and parietal lobe subdivision volumes. The MANCOVA for white matter frontal subdivision analyses was not significant. In contrast the MANCOVA for white matter parietal subdivision analyses was significant;

univariate and post hoc tests revealed that the posterior dorsolateral white matter volumes of the NF1-pure group were larger than those of the control group $F(1, 31) = 3.180, p = .0554$, and the somatosensory white matter volumes of both the NF1-pure and the NF1+ADHD groups were larger than those of the control group $F(1, 31) = 4.823, p = .0150$. The MANCOVA for gray matter frontal subdivision analyses was significant; univariate and post hoc tests revealed that the prefrontal gray matter volumes of the NF1+ADHD group were significantly smaller than the NF1-pure group, $F(1, 31) = 4.592, p = .0179$.

Insert Table 2

Analyses of TWCV, frontal lobe and parietal lobe white matter in UBO +/- groups using the entire NF1 group did not reach significance. However, scatter plots of the data revealed that this was because, as with other findings, the NF1+ADHD group resembled the controls. In order to preliminarily explore if presence of UBOs impacted parietal and frontal white matter volumes, a Robust rank order test was conducted within the NF1-pure group alone, of whom eight had UBOs in the basal ganglia and three did not. This revealed significant differences in TWCV ($p<.05$), parietal white matter ($p<.05$), motor white matter ($p<.01$), frontal deep white matter ($p<.05$), and somatosensory white matter ($p<.05$), such that the white matter of those with UBOs was more markedly enlarged.

Considering data demonstrating abnormal patterns of brain symmetry in idiopathic ADHD[16,17] and other conditions associated with ADHD (i.e. Tourette syndrome),[47,48] we also analyzed asymmetry indices for the four lobes (based on data in table 3). The MANCOVA for this analysis was not significant, indicating similar asymmetry relationships between groups. An additional MANCOVA was also conducted to determine if the lobes for which there were significant differences between groups in gray and white matter were specific to the right or left side. The result of this MANCOVA was significant; univariate and post-hoc tests revealed that significant differences for right parietal white matter (F (1, 31) = 7.828, p = .0018), right frontal white matter (F (1, 31) = 4.488, p = .0194), and both left and right frontal gray matter (F (1, 31) = 4.617, p =.0176 and F (1, 31) = 8.994, p =.0008), with the NF1-pure group showing significantly larger right parietal white matter volumes than the controls. Both NF1 groups (NF1-pure and NF1+ADHD) displayed larger right frontal white matter volumes than the control group with the NF1-pure group exhibiting increases in right frontal gray matter as compared to the NF1+ADHD group. Table 3 displays measurements and analyses of lobar volumes by hemisphere.

Insert Table 3

We extended the above-mentioned analyses to the subdivisions of the frontal and parietal lobes to further localize the lobar hemispheric differences to specific regions, these significant findings are shown in table 4. The MANCOVA for the frontal white matter

subdivisions was significant; univariate and post-hoc tests revealed that the right motor white matter (F (1, 31) = 3.812, p = .0031) and the right premotor white matter (F (1, 31) = 4.554, p = .0184) were larger for the entire NF1 group (both NF1-pure and NF1+ADHD) as compared to controls. The MANCOVA for the parietal white matter subdivisions was significant; univariate and post-hoc tests revealed that the right somatosensory white matter was larger for both the NF1-pure and NF1+ADHD as compared to controls, F (1, 31) = 5.421, p = .0096, and the right dorsolateral parietal white matter and the inferior parietal white matter were larger for the NF1-pure group as compared to controls, F (1, 31) = 4.023, p = .0280 and F (1, 31) = 6.501, p = .0044, respectively. The MANCOVA for the frontal gray matter subdivisions was significant; univariate and post-hoc tests revealed that right prefrontal gray matter was smaller for the NF1+ADHD as compared to NF1-pure, F (1, 31) = 4.307, p = .0224.

Insert Table 4

Discussion

In this study of boys with NF1-pure, NF1+ADHD, and gender-matched normal controls, we confirmed that males with NF1 (NF1-pure and NF1+ADHD) are indeed megalencephalic (larger TCV). This cerebral enlargement appears to be the consequence of larger TWCV and, in particular, larger frontal white matter volume. Moreover, the NF1-pure group was

characterized by the largest TCV, TGCV, and TWCV. The latter was not only due to increased frontal white matter volume, but also represented parietal white matter enlargement. Within this NF1-pure group, a more marked parietal white matter increase was associated with the presence of UBOs in the basal ganglia and thalamus. Among the different parietal subdivisions, the somatosensory white matter seemed to be the main contributor to this UBO-linked enlargement. Although frontal white matter increase in NF1 subjects did not have regional selectivity, NF1-pure males with UBOs had larger motor and frontal deep white matter volumes as compared with their counterparts without UBOs. Co-morbidity with ADHD not only led to a mitigation of parietal increase in NF1 subjects; NF1+ADHD boys had smaller frontal gray matter volumes than NF1-pure subjects, particularly in the prefrontal subdivision. The frontal and parietal white matter increases, as well as the frontal gray matter decrease, mentioned above involved predominantly the right hemisphere. When considering overall findings relevant to NF1, the white matter volume is the predominant contributor to an increase in TCV. However, gray matter volume also contributes to megalencephaly and is decreased only in those individuals with co-morbid ADHD.

The data presented here adds to the growing literature,[9-11] which includes our previous study of a NF1 sample without brain tumors,[8] demonstrating that in NF1 macrocephaly based on head circumference is the result of increased total brain and cerebral volumes. With regard to the controversy about which compartment is responsible for this cerebral enlargement, this work confirms our original hypothesis that the increase in TCV is predominantly secondary to an increase in TWCV. These results are in agreement with two other publications,[10,11] which demonstrate generalized cerebral white matter enlargements. Our analyses have

expanded these observations by showing that the increase in TWCV is not a diffuse process but rather one that involves mainly the frontal and parietal lobes. Discrepancy between our results and a previous report indicating a megalencephaly due to increased gray matter[9] can be explained on the basis of study design. Our investigation focused on cerebral (not brain) measures and included only NF1 males, without tumors or any other major neurologic disturbance, who were classified according to their ADHD status. Co-morbidity of NF1 and ADHD resulted in relative (to NF1-pure) frontal gray matter decrease. This mitigation of frontal enlargement is in agreement with a recent study of the corpus callosum in children with NF1.[12] In the latter, a segment of the corpus callosum was found to be enlarged in NF1 subjects only if ADHD was absent.[12] The mitigation of megalencephaly in NF1, by the presence of co-morbid ADHD, is consistent with literature on males with idiopathic ADHD, which suggests that the pathology underlying ADHD leads to selective frontal[17,18] and, in one study, parietal[18] reductions. Our findings of a predominant right hemispheric change in NF1 are also in line with brain morphometric work on related conditions such as ADHD[17,18,49] and Tourette syndrome[47-49] that demonstrate lateralized findings in a developmental disability.

The association of a greater parietal and posterior frontal white matter enlargement with the presence of UBOs in the centrencephalic region, in the NF1-pure group, supports our hypothesis that UBOs are salient manifestations of a relatively diffuse cerebral white matter abnormality. Evidence in this regard includes a previous MRI study using more sensitive sequences (i.e. FLAIR),[50] which showed the presence of UBOs in multiple white matter regions; a recent report that links reductions in T1 signal with white matter enlargement; and a neuropathologic study that demonstrated vacuolated white matter both in areas of UBOs as

well as diffusely.[25] Our MRSI data on NF1 have also contributed to this view by showing disturbances in NAA and Cho not only in UBO regions, but also more strikingly in the thalamus.[23] In agreement with our postulate that white matter edema is the initial pathologic process in NF1, a recent diffusion weighted imaging investigation showed increased water diffusion in normally appearing cerebral regions including those with UBOs.[24] Furthermore, these authors also demonstrated greater increases in water diffusion in UBO-involved than in normal appearing globus pallidi.[24]

With respect to the dynamics of NF1-associated white matter pathology, our data suggest that the volumetric changes may represent a relatively early event. Most abnormalities involved the right pericentral (posterior frontal/anterior parietal) cortex, which is the oldest cortical region.[51] In addition, white matter growth in NF1 subjects resembled the developmental profiles of control subjects (figure 1). Despite the stability of the volumetric changes, our MRSI data suggest a postnatal process (present already at age 6) of myelin sheath disruption (increased Cho) that leads to axonal injury (reduced NAA) in adolescence (most likely associated with some degree of gliosis).[23] In support of this, there are reports showing T1 hyperintense lesions (UBOs) involving different white matter regions[52] that appear later than and in parallel to T2 UBOs and tend to remain,[53] unlike the better characterized T2 hyperintensities. T1 hyperintensities and the aforementioned reductions in T1 signal[11] have been interpreted as dysplastic myelination or remyelination, which suggests either abnormal myelination or a process of myelin unwrapping followed by "attempts" at repair. Whether remyelination takes place or not, it appears that the end process is axonal damage as

suggested by our MRSI data[23] and by behavioral evaluations demonstrating persistence of neurologic impairment.[54]

In conclusion, our findings provide additional evidence for a cerebral white matter pathologic process in NF1. The volumetric changes appear to be linked to the distinctive hyperintense foci (UBOs), while the relationship between other MR white matter abnormalities (e.g., gliosis, Cho levels) and cerebral enlargement are yet to be determined. The complexity of the pathogenetic process involving the white matter in NF1 is underscored by the recent demonstration that the gene for a major myelin protein, oligodendrocyte myelin glycoprotein (Omgp), is embedded within intron 27b of the NF1 gene.[55] There is also a report of cases of NF1 associated with progressive multiple sclerosis.[56] Consequently, future studies using multiple MR modalities, as well as comprehensive neuroimaging-behavioral correlations, using a longitudinal design are needed to further elucidate the nature and functional repercussion of white matter abnormalities in NF1.

References

1. NIH. National Institutes of Health Consensus Development Conference: Neurofibromatosis Conference Statement. Arch Neurol 1988;45:575-578.

2. Riccardi VM. Von Recklinghausen neurofibromatosis. N Engl J Med 1981;305:1617-1627.

3. North KN. Neurofibromatosis type 1. Am J Med Genet 2000;97:119-127.

4. North KN, Riccardi V, Samango-Sprouse C, et al. Cognitive function and academic performance in Neurofibromatosis Type 1: Consensus statement from the NF1 Cognitive Disorders Task Force. Neurology 1997;48:1121-1127.

5. Stine SB, Adams WV. Learning problems in neurofibromatosis patients. Clin Orthop 1989;245:43-48.

6. Lyon GR, Gray D, Kavanagh J, Krasnegor N, eds. Better understanding Learning Disabilities: New views from research and their implications for education and public policies. Baltimore: Paul H. Brookes, 1993.

7. Denckla MB, Hofman K, Mazzocco MM, et al. Relationship between T2-weighted hyperintensities (unidentified bright objects) and lower IQs in children with neurofibromatosis. Am J Med Genet 1996;67:98-102.

8. Cutting LE, Koth CW, Burnette CP, Abrams MT, Kaufmann WE, Denckla MB. Relationship of cognitive functioning, whole brain volumes, and T2 weighted hyperintensities in neurofibromatosis-1. J Child Neurol 2000;15:157-160.

9. Moore BD, Slopis JM, Jackson EF, DeWinter AE, Leeds NE. Brain volume in children with neurofibromatosis type 1: relation to neuropsychological status. Neurology 2000; 54:914-920.

10. Said SM, Yeh TL, Greenwood RS, Whitt JK, Tupler LA, Krishnan KR. MRI morphometric analysis and neuropsychological function in patients with neurofibromatosis. Neuroreport 1996;7:1941-1944.

11. Steen RG, Taylor JS, Langston JW, Glass JO, Brewer VR, Reddick WE, Mages R, Pivnick EK. Prospective evaluation of the brain in asymptomatic children with neurofibromatosis type 1: relationship of macrocephaly to T1 relaxation changes and structural brain abnormalities. AJNR Am J Neuroradiol 2001;22:810-817.

12. Kayl AE, Moore BD, Slopis JM, Jackson EF, Leeds NE. Quantitative morphology of the corpus callosum in children with neurofibromatosis and attention-deficit hyperactivity disorder. J Child Neurol 2000;15,90-96.

13. Koth CW, Cutting LE, Denckla MB. The association of neurofibromatosis type 1 and attention deficit hyperactivity disorder. Child Neuropsychology in press.

14. Mautner VF, Thakkar SD, Kluwe L, Leark RA. Treatment of attention deficit hyperactivity disorder in neurofibromatosis type 1. Presented at the 23rd Annual Mid-Year Meeting of the International Neuropsychological Society; 2000; Brussels.

15. Zametkin AJ, Ernst M. Problems in the management of attention-deficit-hyperactivity disorder. N Engl J Med 1999;340:40-46.

16. Aylward EH, Reiss AL, Reader MJ, Singer HS, Brown JE, Denckla MB. Basal ganglia volumes in children with attention deficit hyperactivity disorder. J Child Neurol 1996;11:112-115.

17. Castellanos FX, Geidd JN, Marsh WL, et al. Quantitative brain magnetic resonance imaging in attention deficit hyperactivity disorder. Arch Gen Psychiatry 1996;53:607-616.

18. Filipek PA, Semrud-Clikeman M, Steingard RJ, Renshaw PF, Kennedy DN, Biederman J. Volumetric MRI analysis comparing subjects having attention deficit hyperactivity disorder with normal controls. Neurology 1997;48:589-601.

19. Giedd JN, Castellanos FX, Casey BJ, et al. Quantitative morphometry of the corpus callosum in attention deficit hyperactivity disorder. Am J Psychiatry 1994;151:665-669.

20. Berquin PC, Giedd JN, Jacobsen LK, et al. Cerebellum in attention-deficit hyperactivity disorder: a morphometric MRI study. Neurology 1998; 50:1087-1093.

21. Mostofsky SH, Reiss AL, Lockhart P, Denckla MB. Evaluation of cerebellar size in attention deficit hyperactivity disorder. J Child Neurol 1998;13:434-439.

22. Castellanos FX, Giedd JN, Berquin PC, et al. Quantitative brain magnetic resonance imaging in girls with attention deficit hyperactivity disorder. Arch Gen Psychiatr 2001; 58:289-295.

23. Wang PY, Kaufmann WE, Koth CW, Denckla MB, Barker PB. Thalamic involvement in neurofibromatosis type 1: evaluation with proton magnetic resonance spectroscopic imaging. Ann Neurol 2000;47:477-484.

24. Eastwood JD, Fiorella DJ, MacFall JF, Delong DM, Provenzale JM, Greenwood RS. Increased brain apparent diffusion coefficient in children with neurofibromatosis type 1. Radiology 2001;219:354-358.

25. DiPaolo DP, Zimmerman RA, Rorke LB, Zackai EH, Bilaniuk LT, Yachnis AT. Neurofibromatosis type1: pathologic substrate of high-signal-intensity foci in the brain. Radiology 1995;195:721-724.

26. Welner Z, Reich W, Herjanic B, Jung KG, Amado H. Reliability, validity, and parent-child agreement studies of the Diagnostic Interview for Children and Adolescents (DICA). J Am Acad Child Adolesc Psychiatry 1987;26:649-653.

27. American Psychiatric Association. Diagnostic and Statistical Manual of Mental Disorders, 3rd ed., revised. Washington, DC: American Psychiatric Association, 1987

28. Dupaul GJ. Parent and teacher ratings of ADHD symptoms: Psychometric properties in a community based sample. J Clin Child Psychol 1991;20:243-253.

29. American Psychiatric Association. Diagnostic and Statistical Manual of Mental Disorders, 4th ed. Washington, DC: American Psychiatric Association, 1994.

30. Achenbach T. Child Behavior Checklist (Parent Form). Burlington, VT: University Associates in Psychiatry, 1991.

31. Conners KC. Conners' Rating Scales – Revised – Parent Version. North Tonawanda, NY: Multihealth Systems, Inc., 1989.

32. Wechsler DL. The Wechsler Intelligence Scale for Children – Revised. San Antonio, TX: The Psychological Corporation, 1974.

33. Wechsler DL. Wechsler Adult Intelligence Scale – Revised. San Antonio, TX: The Psychological Corporation, 1981.

34. Wechsler DL. The Wechsler Intelligence Scale for Children – III. San Antonio, TX: The Psychological Corporation, 1991.

35. Thorndike RL, Hagen EP, Sattler JM. The Stanford-Binet Intelligence Scale: Fourth Edition. Chicago, IL: Riverside Publishing, 1986.

36. Behavioral Neurogenetic and Neuroimaging Research Center, BrainImage. (2.5.x) Baltimore: Kennedy Krieger Institute, 1997.

37. Subramaniam B, Hennessey JG, Rubin MA, Beach LS, Reiss AL. Software and methods for quantitative imaging in neuroscience: The Kennedy Krieger Institute Human Brain Project. In: Koslow SH, Huerta MF, eds. Neuroinformatics: an overview of the human brain project. Manwah, NJ: Lawrence Erlbaum, 1997.

38. Reiss AL, Hennessey JG, Rubin M, et al. Reliability and validity of an algorithm for fuzzy tissue segmentation of MRI. J Comp Assist Tomogr 1998;22;471-479.

39. Talairach J, Tournoux P, eds. Co-planar stereotaxic atlas of the human brain. New York: Thieme Medical Publishers, Inc., 1988.

40. Andreasen NC, Rajarethinam R, Cizadlo T, et al. Automatic atlas-based volume estimation of human brain regions from MR images. J Comp Assist Tomogr 1996;20:98-106.

41. Kaplan DM, Liu AM, Abrams MT, et al. Application of an automatic parcellation method to the analysis of pediatric brain volumes. Psychiatry Res 1997;76:15-27.

42. Kates WR, Warsofsky IS, Patwardhan A, et al. Automated Talairach atlas-based parcellation and measurement of cerebral lobes in children. Psychiatry Res 1999;91:11-30.

43. Reiss AL, Abrams MT, Singer HS, Ross JL, Denckla MB. Brain development, gender and IQ in children. A volumetric imaging study. Brain 1996;119:1763-74.

44. Giedd JN, Snell JW, Lange N, et al. Quantitative magnetic resonance imaging of human brain development: ages 4-18. Cereb Cortex 1996;6:551-560.

45. Giedd JN, Blumenthal J, Jeffries NO, et al. Brain development during childhood and adolescence: a longitudinal MRI study. Nat Neurosci 1999;2:861-863.

46. Games PA, Howell JF. Pairwise multiple comparison procedures with equal n's and/or variances: A monte carlo study. J Educ Stat 1976;1:113-125.

47. Singer HS, Reiss AL, Brown JE, et al. Volumetric MRI changes in basal ganglia of children with Tourette's syndrome. Neurology 1993;43:950-956.

48. Castellanos FX, Giedd JN, Hamburger SD, Marsh WL, Rapoport JL. Brain morphometry in Tourette's syndrome: the influence of comorbid attention deficit/hyperactivity disorder. Neurology 1996;47:1581-1583.

49. Baumgardner TL, Singer HS, Denckla MB, et al. Corpus callosum morphology in children with Tourette syndrome and attention deficit hyperactivity disorder. Neurology 1996;47:1-6.

50. Yamanouchi H, Kato T, Matsuda H, Takashima S, Sakuragawa N, Arima M. MRI in neurofibromatosis type I: using fluid-attenuated inversion recovery pulse sequences. Pediatr Neurol 1995;12:286-290.

51. Kaufmann WE (2001) Cortical histogenesis. In: Aminoff MJ, Daroff RB, eds. Encyclopedia of the Neurological Sciences. Section on Neuroanatomy & Clinical Localization (Masdeu JC, ed.). New York: Academic Press: in press.

52. Mirowitz SA, Sartor K, Gado M. High-intensity basal ganglia lesions on T1-weighted MR images in neurofibromatosis. Am J Roentgenol 1990;154:369-373.

53. Terada H, Barkovich AJ, Edwards MS, Ciricillo SM. Evolution of high-intensity basal ganglia lesions on T1-weighted MR in neurofibromatosis type 1. Am J Neuroradiol 1996;17:755-760.

54. Cutting LE, Koth CW, Gua-Guang H, Zeger SL, Denckla MB. Growth curve analyses of neuropsychological profiles of children with neurofibromatosis type 1: specific cognitive functions remain "spared" and "impaired" over time. J Neuropsychological Soc 2001:submitted.

55. Habib AA, Gulcher JR, Hognason T, Zheng L, Stefansson K. The OMgp gene, a second growth suppressor within the NF1 gene. Oncogene 1998;16:1525-1531.

56. Johnson MR, Ferner RE, Bobrow M, Hughes RA. Detailed analysis of the oligodendrocyte myelin glycoprotein gene in four patients with neurofibromatosis 1 and primary progressive multiple sclerosis. J Neurol Neurosurg Psychiatry 2000;68:643-646.

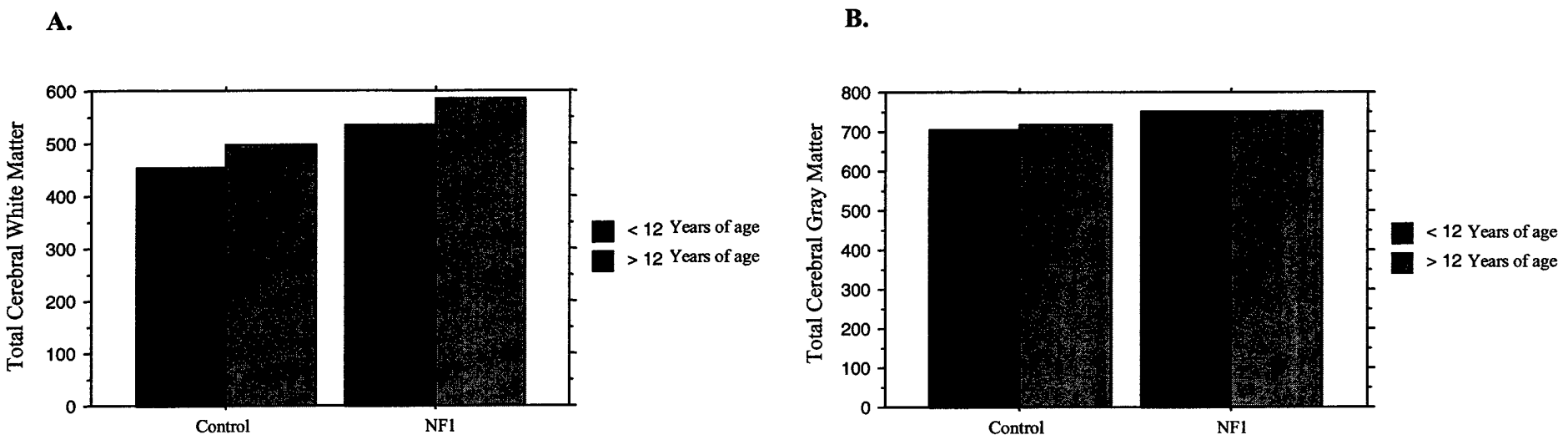

Figure 1. A. The bar chart compares total Cerebral White matter volumes (TWCV) of the entire NF1 group, including those with and without ADHD, and their age-matched controls. **B.** The bar chart compares total Cerebral Gray matter volumes (TGCV) of the entire NF1 group, including those with and without ADHD, and their age-matched controls.

Table 1. Cerebral and lobar volumes in NF1 subjects and controls

	NF1- pure (N=11)	NF1+ ADHD (N=7)	Controls (N=18)
Total Cerebral Volume	1370.943 ± 147.876 §	1217.402 ± 52.653	1186.073 ± 101.160
Total Cerebral Gray Matter	789.656 ± 77.436 §	691.404 ± 24.425	709.937 ± 65.749
Total Cerebral White Matter	581.287 ± 82.166 ‡	526.000 ± 41.702 ‡	476.136 ± 47.324
Frontal Gray Matter*	278.213 ± 27.764 †	242.778 ± 10.484	254.825 ± 24.820
Frontal White Matter*	225.355 ± 36.489 ‡	203.037 ± 17.364 ‡	182.265 ± 19.111
Parietal Gray Matter*	191.457 ± 22.625	169.814 ± 12.523	172.051 ± 16.780
Parietal White Matter*	162.207 ± 20.652 ‡	146.179 ± 14.884	132.726 ± 13.574
Temporal Gray Matter*	176.185 ± 16.440	150.375 ± 8.540	152.728 ± 16.917
Temporal White Matter*	78.655 ± 12.625	74.804 ± 4.371	65.335 ± 11.695
Occipital Gray Matter*	97.119 ± 12.431	82.613 ± 5.883	83.437 ± 8.907
Occipital White Matter*	62.090 ± 10.291	54.513 ± 7.889	52.315 ± 7.250

All values reported as means ± standard deviation.

All analyses used age as a covariate.

* Covaried for Total Cerebral Volume

† $p < 0.01$, relative to NF1+ADHD

‡ $p < 0.02$, relative to Controls

§ $p < 0.01$, relative to both NF1+ADHD and Controls

Table 2. Frontal and Parietal lobe subdivision volumes in NF1 subjects and controls

	NF1- pure (N=11)	NF1+ ADHD (N=7)	Controls (N=18)
Frontal Subdivisions			
Prefrontal Gray Matter	139.782 ± 15.770†	117.730 ± 11.904	125.789 ± 13.924
Prefrontal White Matter	76.789 ± 18.660	65.412 ± 7.612	57.530 ± 7.660
Premotor Gray Matter	62.015 ± 7.062	54.923 ± 2.013	56.535 ± 5.726
Premotor White Matter	30.959 ± 6.120§	29.856 ± 3.416§	25.200 ± 3.887
Motor Gray Matter	33.158 ± 4.052	30.049 ± 1.625	29.551 ± 2.979
Motor White Matter	24.694 ± 3.755‡	22.854 ± 2.628	20.099 ± 2.871
Frontal Deep White Matter	63.236 ± 7.726	57.063 ± 4.480	53.818 ± 4.843
Anterior Cingulate Gray Matter	17.030 ± 1.723	15.472 ± 1.912	16.048 ± 2.459
Anterior Cingulate White Matter	19.655 ± 3.471	18.545 ± 2.130	16.652 ± 2.386
Parietal Subdivisions			
Somatosensory Gray Matter	36.257 ± 4.976	32.438 ± 2.908	31.747 ± 2.976
Somatosensory White Matter	20.125 ± 2.845	18.595 ± 1.683	16.117 ± 2.007
Dorsolateral Gray Matter	52.894 ± 6.903	45.657 ± 3.458	44.519 ± 6.019
Dorsolateral White Matter	25.775 ± 4.764	21.924 ± 4.494	19.110 ± 2.922
Inferior Parietal Gray Matter	61.301 ± 7.916	52.675 ± 5.699	53.487 ± 5.487
Inferior Parietal White Matter	35.680 ± 6.129	31.563 ± 3.747	28.023 ± 3.368
Parietal Deep White Matter	56.560 ± 6.102	52.166 ± 4.209	49.539 ± 5.137
Posterior Cingulate Gray Matter	14.123 ± 2.515	13.210 ± 2.060	14.476 ± 2.523
Posterior Cingulate/ Corpus Callosum White Matter	17.489 ± 2.605	16.183 ± 2.026	14.836 ± 1.918

All values reported as means ± standard deviation.

All analyses used age and Total Cerebral Volume as covariates.

† $p < 0.03$, relative to NF+ADHD

‡ $p < 0.01$, relative to Controls

§ $p < 0.04$, relative to Controls

Table 3. Lobar volumes for left and right hemispheres in NF1 subjects and controls

	NF1- pure (N=11)	NF1+ ADHD (N=7)	Controls (N=18)
Frontal Gray Matter			
Left	134.732 ± 15.710 †	117.561 ± 5.650	122.630 ± 13.128
Right	143.484 ± 13.325 †	125.215 ± 5.912	132.194 ± 12.253
Frontal White Matter			
Left	111.588 ± 18.672	101.401 ± 11.701	91.295 ± 9.276
Right	113.766 ± 18.021 ‡	101.636 ± 7.982 ‡	90.968 ± 11.015
Parietal Gray Matter			
Left	93.403 ± 11.411	83.016 ± 6.649	85.148 ± 8.486
Right	98.055 ± 11.825	86.798 ± 6.627	86.902 ± 8.607
Parietal White Matter			
Left	80.442 ± 12.332	72.991 ± 7.551	66.408 ± 8.123
Right	81.764 ± 8.604	73.184 ± 7.452	66.318 ± 5.904
Temporal Gray Matter			
Left	87.781 ± 9.061	74.154 ± 4.590	74.917 ± 9.172
Right	88.404 ± 8.156	76.227 ± 4.048	77.812 ± 8.004
Temporal White Matter			
Left	39.641 ± 6.385	37.574 ± 1.762	32.962 ± 6.303
Right	39.014 ± 6.794	37.229 ± 3.255	32.372 ± 5.795
Occipital Gray Matter			
Left	47.851 ± 6.434	41.114 ± 3.496	41.826 ±4.425
Right	49.267 ± 6.437	41.499 ± 3.083	41.611 ± 4.885
Occipital White Matter			
Left	32.370 ± 5.752	26.940 ± 4.012	25.957 ± 4.527
Right	29.720 ± 4.964	27.571 ± 4.684	26.358 ± 3.505

All analyses used age and Total Cerebral Volume as covariates, values reported as means ± standard deviation.

† $p < 0.01$, relative to NF+ADHD, ‡ $p < 0.02$, relative to Controls

Table 4. Hemispheric findings in the frontal and parietal lobe subdivision volumes NF1 subjects and controls

	NF1- pure (N=11)	NF1+ ADHD (N=7)	Controls (N=18)
Frontal Subdivisions			
Right Prefrontal Gray Matter	72.309 ± 7.572	61.525 ± 6.035	65.780 ±7.088
Right Premotor White Matter	15.516 ± 3.092‡	15.243 ± 2.007‡	12.304 ± 2.345
Right Motor White Matter	12.728 ± 1.898†	11.649 ± 1.460	10.202 ± 1.594
Parietal Subdivisions			
Right Somatosensory White Matter	10.067 ± 1.359†	9.311 ± .679†	8.020 ± 1.066
Right Dorsolateral Parietal White Matter	12.927 ± 2.433‡	11.220 ± 2.392	9.526 ± 1.480
Right Inferior Parietal White Matter	18.350 ± 2.422†	15.675 ± 1.957	13.908 ± 1.575

All values reported as means ± standard deviation.

All analyses used age and Total Cerebral Volume as covariates.

† $p < 0.01$, relative to Controls

‡ $p < 0.03$, relative to Controls

Longitudinal Evolution of T2-Weighted Hyperintensities in Children with Neurofibromatosis-1

Michael A. Kraut,[1*] Joan P. Gerring,[2,3,4] Karen L. Cooper,[4] Richard E. Thompson,[5]

Martha B. Denckla[2,3,4,6] and Walter E. Kaufmann[1,2,3,4,6,7]

[1]Department of Radiology and Radiological Science, Johns Hopkins University School of Medicine, Baltimore, Maryland
[2]Department of Psychiatry and Behavioral Sciences, Johns Hopkins University School of Medicine, Baltimore, Maryland
[3]Department of Pediatrics, Johns Hopkins University School of Medicine, Baltimore, Maryland
[4]Kennedy Krieger Institute, Baltimore, Maryland
[5]Department of Biostatistics, Bloomberg School of Public Health, Johns Hopkins University
[6]Department of Neurology, Johns Hopkins University School of Medicine, Baltimore, Maryland
[7]Department of Pathology, Johns Hopkins University School of Medicine, Baltimore, Maryland

Running Title: UBO evolution in Neurofibromatosis-1

* Correspondence to:
Michael A. Kraut, M.D., Ph.D.
Department of Radiology and Radiological Science
Johns Hopkins Hospital
600 N Wolfe St, Houck B-112
Baltimore, MD 21287
E-mail: mkraut@rad.jhu.edu

(ABSTRACT)

Neurofibromatosis type-1 (NF-1) is the most common autosomal dominant disorder affecting the central nervous system. Magnetic resonance imaging (MRI) has revealed distinctive T2-weighted hyperintense lesions (termed UBOs), which appear to represent spongiform changes in the white matter. Cross-sectional and longitudinal analyses suggest that UBOs disappear over time; however, none of these studies have examined comprehensively these lesions. We conducted a quantitative MRI longitudinal study of number of affected regions, number of UBOs per region, and UBO volume per region, in a sample of 12 children with NF-1. We applied semi-automatic morphometric methods and comprehensive statistical approaches, within a detailed anatomical parcellation framework. Our data demonstrate that, despite a similar UBO regional distribution (e.g., prevalent globus pallidus/internal capsule location), lesion evolution was more complex than previously reported. The total number of UBO-occupied locations evolved in a non-linear manner, with a decrease between approximately ages 7-12 years, followed by a progressive increase during adolescence. This pattern was also found for UBO number and/or volume for all regions, with the exception of the cerebellar hemispheres. This distinction may reflect differences in white matter structure between affected long tract fiber bundles and that of cerebral and cerebellar myelinated fibers. The findings are also discussed in the context of previous MR and behavioral studies. We conclude that studies like the present one, in association with other MR modalities, are necessary to characterize more completely the nature and evolution of UBOs and their role in the cognitive phenotype of NF-1.

Key Words: Neurofibromatosis-1, UBO, MRI, evolution

INTRODUCTION

Neurofibromatosis type-1 (NF-1) is the most common autosomal dominant disorder affecting the central nervous system [Riccardi, 1999]. Since the earliest magnetic resonance imaging (MRI) studies of patients with NF-1 [Brown et al., 1987; Hurst et al., 1988; Aoki et al., 1989; Goldstein et al., 1989], investigators have noted the presence of T2-weighted hyperintense lesions (T2W), also termed unidentified bright objects (UBOs), most often found in the deep gray structures, the brainstem, and the cerebellum. The histologic nature of the lesions remains obscure, although the limited available pathologic material suggests that the signal abnormalities reflect spongiform changes in the white matter [DiPaolo et al., 1995], compatible predominantly with intramyelinic edema. At least two groups have evaluated the evolution of these lesions over time [Itoh et al., 1994; DiMario and Ramsby, 1998], and have found that, in general, the lesion burden tends to decrease over time, but that the patterns of change over time vary by brain region. In one of the previous studies, in which patients were examined serially, seven patients were studied at more than two time points [DiMario and Ramsby, 1998]. Those results were reported in a framework of an anatomic parcellation in which the locations of all the lesions were assigned to cerebral hemisphere, brainstem (diencephalic lesions were included in this compartment) or cerebellum; using this parcellation scheme, the lesions were found to occur most often in the cerebellum and in the globus pallidus. The authors alluded to the fact that their data showed an increase in the number and size of brainstem lesions over the course of several years, while the lesion burden in the cerebral hemispheres and the cerebellum decreased. In the other

study, Itoh et al. [1994] serially studied 13 patients as part of a larger investigation into the evolution of the NF-1-related lesions. In that study, the anatomic distinctions were somewhat finer, with five compartments (basal ganglia, brainstem, dentate nuclei, cerebellar white matter, cerebral white matter) to which lesions could be assigned. They found the lesions occur most frequently in the basal ganglia and in the brainstem and that, with time, the overall tendency was for the lesions to decrease in size. The methods used to characterize the time-dependent behavior of the lesions were not well described in either study. Also, while the study by Itoh et al. [1994] characterized the lesion evolution in terms of lesion volume, the DiMario and Ramsby's report focused on region specific lesion number and maximal cross sectional area, without explicit calculation of lesion volumes. Furthermore, postmortem [DiPaolo et al., 1995] and MRI [Said et al., 1996; Steen et al., 2001] studies have emphasized the importance of white matter involvement in NF-1, including the fact that UBOs appear to be distributed along major white matter tracts [Yamanouchi et al., 1995]. The latter data, in conjunction with our own observations, suggest that the distribution and evolution of UBOs should be analyzed in a scheme of anatomical parcellation that accounts for white matter fiber bundles that originate or terminate at, or pass through, the regions being evaluated.

The goal of this study was to analyze these NF-1 lesions longitudinally, in a pediatric sample with predominantly more than two observations and within a higher-resolution MRI anatomic framework, in order to characterize more accurately both their spatial distribution and the time course of their evolution. Since some aspects of the behavioral deficits exhibited by NF-1 patients, specifically the lowering of IQ relative to

unaffected siblings, appear to correlate with the number of regions involved by UBOs [Denckla et al., 1996], the present investigation examined all three variables, i.e., number of lesions, size of lesions, and number of regions affected by these UBOs. Determining similarities and differences in the time courses of region-specific lesion number and lesion volume would be helpful in not only characterizing the neuroanatomical bases of the behavioral abnormalities exhibited by children with NF-1, but also would shed some light into the nature of the underlying pathogenetic process. For instance, changes in the number of regions involved by UBOs would provide information about the multifocal nature of the process. The relationship between number and size of lesions would also help to elucidate whether UBOs are discrete entities or represent the visible manifestation of a more diffuse process. We postulate that this information, in the context of a detailed anatomical framework, will contribute to both more informative lesion-deficit correlations and better clinical prognostication in NF-1.

MATERIAL AND METHODS

Population and Procedures

We obtained 34 examinations on twelve patients (eleven males, one female) with NF-1, ranging in age from about 7.1 to about 19.5 years, with an average (+/- s.d.) age of 13.0 +/- 3.3 years and average full scale IQ of 105.0 +/- 12.3. Five subjects were evaluated at two time points, four subjects at three time points, and three at four time points. The mean number of scans/subjects was 2.8, and the mean time interval between scans was 2.0 +/- 0.8 years. Five subjects were diagnosed with sporadic NF-1 and seven were diagnosed with familial NF-1.

The subjects were recruited as part of a larger research-center-based investigation of genetic and learning disabilities, "Neurodevelopmental Pathways to Learning Disabilities", at the Kennedy Krieger Institute in Baltimore, Maryland. Children affected with either familial or sporadic NF-1 were diagnosed based on the National Institutes of Health consensus criteria [NIH. National Institutes of Health Consensus Development Conference, 1988]. Subjects were excluded if they had any intracranial pathology such as optic gliomas and/or other brain tumors, history of seizures, or any significant uncorrectable hearing or visual impairments. Cognitive ability was assessed with the Wechsler Intelligence Scale for Children [Wechsler 1974, 1991] at the time of the first MRI scan. Nine children were assessed with the Wechsler Intelligence Scale for

Children- revised version (WISC-R) and three were assessed with the Wechsler Intelligence Scale for Children- III (WISC-III).

MRI Acquisition

All scans were performed on a 1.5 T General Electric Signa Scanner (Milwaukee, Wisconsin) using the standard GE quadrature head coil. Three axial series were obtained parallel to the anterior-posterior (AC-PC) intercommissural line: a T1-weighted sequence (TR/TE=500-600/20), as well as the proton density (PD) and T2-weighted (T2W) sequences (TR/TE = 3000/30,100 ms) that were used for lesion evaluation. All series were gathered as 5 mm thick interleaved images with a field of view of between 22-24 cm. The imaging data were then post-processed to reduce systematic inhomogeneities within and between scan sections as previously described [Denckla et al., 1996].

MRI Post-Acquisition Analysis

The lesions, defined operationally as regions of confluent hyperintensity (signal intensity higher than that of cortical gray matter) on the PD and the T2W images without associated mass effect, were initially identified by visual inspection by two of the authors independently. For each imaging section in which lesions were detected, UBOs were initially manually delineated, followed by a seed-based automatic segmentation algorithm that provided the final outline of the lesion [Itoh et al., 1994; Denckla et al., 1996]. Because of the complex three-dimensional configuration of UBOs, we used the

operational designation of independent lesion for every abnormality observed on every single MRI slice. This UBO definition was used for both number and volume measurements. The lesions were assigned to one of eighteen pre-defined anatomic regions (Table I), reflecting both the patterns of lesion distribution in previous reports [Aoki et al., 1989; Itoh et al., 1994; Yamanouchi et al., 1995; Steen et al., 2001], as well as in our data. If a lesion crossed regional boundaries, it was counted or measured in each of the locations. These regions assignments were reviewed, and any uncertainties regarding anatomic localization were resolved by adjudication between two of the authors, one of whom is a Neuroradiologist (MAK) and the other a Neuropathologist (WEK).

Insert Table I about here

Since the number of lesions per hemisphere was approximately the same for all regions (see Results), for all analyses the left and right hemispheres were combined. Number of lesions represented the count of independent lesions per each one of the eighteen regions, under evaluation, as defined above. Preliminary examination of these raw data demonstrated that UBOs were rather infrequent in some of the original locations. In addition, distinction between UBOs in the globus pallidus and internal capsule was rather difficult in many instances. Therefore, original regions were combined into clusters representing locations with similar function and/or containing

different portions of the same fiber bundle system. In this way, the final analyses of number of locations, number of UBOs, and UBO volume were conducted on the following regional groups: (1) striatal region: caudate, putamen, claustrum, external capsule; (2) globus pallidus, internal capsule; (3) diencephalic region: thalamus, hypothalamus, subthalamus; (4) medial cerebellar region: cerebellar vermis, deep cerebellar nuclei, middle cerebellar peduncle; (5) ventral midbrain (cerebral peduncle), ventral pons; and (6) dorsal midbrain, pontine tegmentum, medulla. Because of the relatively large number of lesions, the (lateral) cerebellar hemispheres (mainly white matter) were analyzed as a single entity. From this scheme, number of locations was defined as the total number of any of the seven clusters/region occupied by UBO(s) per MRI examination. Volumetric assessments were done by reconstruction of a volume of interest (VOI) as described in earlier studies [Itoh et al., 1994; Denckla et al., 1996]. Each VOI (in cc) represented the addition of all UBO volumes within a given anatomical region (the seven clusters/regions mentioned above); in other words, it did not correspond to the volume of a single lesion but rather to the combined volume of one or more UBOs per location. Figure 1 depicts UBOs in the frequent globus pallidus/internal capsule location.

Insert Figure 1 about here

Statistical Plan and Analysis

All analyses were preformed using STATA 6.0.

Number of locations and UBOs. We postulate that number of locations would reflect the severity and dynamics (e.g., progressive or static) of the pathophysiologic process. Complementing the latter, number of lesions per specific location would represent the regional propensity for UBO formation and, to some extent, the "activity" of the process. Both continuous variables were analyzed by a Poisson regression analysis, in which the outcome is the incidence rate of the event. In this case, the incidence is the number of locations per subject, or the number of UBOs, expressed as a function of age and age^2. The incidence rate for an individual j can be expressed in general terms as:

$$r_j = \exp(\beta_0 + \beta_1 age_j + \beta_2 age_j{}^2)$$

where the regression beta coefficients are estimated from the data. Because we have multiple measurements taken on the individual patients, the method of general estimating equations (GEE) was used with the STATA procedure command *xtgee* and the Poisson distribution specified. The ratio of the incidence rates allows us to calculate incidence rate ratios (IRR) between two individuals. For instance, we may want to know whether a one-year increase in age increases or decreases the expected number of locations or UBOs. In the case of the cerebellar hemispheres, the incidence rate was found to be linear in age only with a decrease in expected UBOs over time (e.g., ß$_2$ in the above equation is statistically equal to zero), giving a incidence rate ratio for each one-year increase as:

IRR = exp(-0.4247) = 0.654,

where –0.4247 is our estimated value for β_1 in the above equation.

This tells us that the expected rate of UBOs for a given patient is 0.654 times that of another patient that is one year younger, regardless of the ages being compared.

In the cases where the quadratic term in age is significant, then the actual ages being compared effects the estimated IRR. For example, the non-linear incidence rate of UBOs in the globus pallidus/internal capsule region (see Fig. 4) produced an IRR for an 11 year old versus a 10 year of 0.861, and an IRR for a 17 year old versus a 16 year old as 1.154. Thus, a one year increase in age from 10 to 11 results in a lower expected number of UBOs, while a year increase in age from 16 to 17 results in an increase in the expected number of UBOs according to the regression model.

UBO volume: We hypothesize that region-wise volume of lesion would reflect the magnitude of the spongiform change and the degree to which the lesions would cause local neural dysfunction. Preliminary scatter plots of UBO volumes on age fitted with a smoothing spline, suggesting that UBO volumes are not linear with age, but instead are high at younger ages, decrease into the early teenage years, and then increase again in the later teen years. Therefore, lesion volumes for a given location were regressed on linear and quadratic terms in age (e.g., independent variables of age and age^2) as suggested by the data pattern in the scatter plots. The regression model can be written in general terms as:

$$total\,volume = \beta_0 + \beta_1 age + \beta_2 age^2$$

where the regression beta coefficients are estimated from the data. As for the counts described above, the GEE was used with the STATA procedure command *xtgee* that allowed to estimate the regression coefficients and corresponding standard errors of these coefficients while taking into account possible correlations in UBO volumes within the individual.

RESULTS

Regional distribution of T2W hyperintense lesions

The 34 MRI examinations in our 12 subjects demonstrated a total of 393 UBOs, as defined in the Methods section, in the regions under analyses. The number of lesions in other locations was substantially lower. The most frequent location was the globus pallidus/internal capsule with a total of 210 lesions (left, 94; right 116). The second most common locations were the diencephalic and medial cerebellar regions, with 43 lesions each (left, 16; right 27; and left, 23; right, 20, respectively). The cerebellar cortex showed 34 UBOs (left, 21; right, 13), while the total number of lesions in the striatal cluster was 30 (left, 19; right, 11). Finally, the combined count of lesions for the two brainstem regional groups was 33 (left, 18; right, 15).

Number of locations affected by T2W hyperintense lesions

Analysis of the number of clusters with at least one UBO, as a function of age, showed a non-linear trend. The number of affected regions was initially high (approximately 5), decreased during the pre-teen years (between ages 5 and about 13 years to an approximate mean of 2.5), and increased again in the late teens to a level comparable to early childhood. Figure 2 illustrates this evolution.

Insert Figure 2 about here

Numbers of T2W hyperintense lesions

As mentioned in the preceding Methods section, we found two distinct patterns of lesion appearance/regression into which lesion number segregate. In the cerebellar vermis, deep cerebellar nuclei, middle cerebellar peduncle cluster, as well as in the cerebellar hemispheric white matter, the number of lesions drops sharply from between the ages of 5 and 10 years, and remains small thereafter. Data demonstrating this pattern is shown in Figure 3. In all other locations, UBO number demonstrates the same non-linear pattern of evolution shown by the number of involved regions (see preceding section and Fig. 2). There was an initial pre-teen decrease followed by a similar increase between approximately ages 13 and 19 years. This prevalent pattern is exemplified by the location with largest numbers of UBOs, the globus pallidus/internal capsule, which is depicted in Figure 4.

Insert Figure 3 about here

Insert Figure 4 about here

Volume of T2W hyperintense lesions

In the case of total UBO volume per region, most locations showed a definite non-linear trend in age, where lesion volume was initially high, decreased between ages 7 and 12-14 years, and increased again thereafter. As with the number of UBOs, an exception to this rule was the region of the cerebellar hemispheres. The regression analyses demonstrated that UBO volume was linear with age, with a statistically significant decrease as the patients get older. In the striatal region, neither the age nor the age^2 coefficients met strictly the criteria for statistical significance, but the covariates closely approached significance with corresponding p-values of 0.051 and 0.052 for age and age^2, respectively. Figures 5 and 6 illustrate the linear and non-linear patterns, by depicting UBOs volume for the cerebellar hemispheres and the globus pallidus/internal capsule, respectively.

Insert Figure 5 about here

Insert Figure 6 about here

DISCUSSION

Our data demonstrate the same overall regional distribution of the characteristic T2W hyperintense foci reported by previous studies in children with NF-1. The globus pallidus/internal capsule was the most common location, with substantially fewer lesions in the diencephalic, medial cerebellar, hemispheric cerebellar, and striatal regions. Only the number of UBOs in the brainstem was relatively smaller than earlier reports [DiMario and Ramsby, 1998]. Despite this general agreement, we found a different and complex pattern of evolution of UBOs. In terms of the number of affected regions, UBOs are initially found in most of the examined locations (i.e., approximately 5 out 7 regions). This is followed by a decrease to a minimum (approximately 2.5 regions) during the pre-teen years, and a progressive increase to earlier childhood levels after age 12-14 years. This non-linear evolution is also observed for both the number of lesions per region and the total volume occupied by UBOs in a given region, in most locations. Interestingly, not only the pattern but also the specific ages mentioned above are similar for most of the parameters. A distinct exception to this pattern of longitudinal evolution was evident in the cerebellar hemispheres, which showed a statistically significant decrease in both lesion number and volume as the patients got older. Additionally, the number of lesions in the medial cerebellar structures (i.e., cerebellar vermis, deep cerebellar nuclei, middle cerebellar peduncle), displayed a linear reduction over time, while UBO volume in the striatal region (caudate, putamen, claustrum, external capsule) showed a trend approaching significance towards non-linear evolution ($p = 0.052$ for age^2).

The data presented here provide, to our knowledge, the first evidence of a complex pattern of evolution for T2W hyperintense foci in children with NF-1. These lesions have been recognized as a distinctive feature of NF-1 since the late 1980s, and have recently been incorporated into the diagnostic criteria of NF1 [Gutmann et al., 1997]. Cross-sectional analyses, and more recently longitudinal evaluations, indicate that UBOs tend to regress during adolescence [Itoh et al., 1994, DiMario and Ramsby, 1998; North, 2000]. The first major serial study of UBOs included 13 subjects with two observations each, and assessed volume of lesions in five locations: cerebral white matter, basal ganglia, brainstem, dentate nucleus, and cerebellar white matter [Itoh et al., 1994]. In 7/13 subjects, UBOs disappeared or decreased; two individuals showed no change, and 3 subjects had new or larger lesions. Interestingly, in this study, one NF-1 subject showed UBO volume increase in the basal ganglia and reduction in the brainstem and cerebral white matter [Itoh et al., 1994]. These data suggest that while the predominant pattern is one of decrease, there are NF-1 patients who may experience appearance or enlargement of UBOs. A second serial investigation incorporated a true longitudinal component, with 7/15 patients with more than two MRI scans over time [DiMario and Ramsby, 1998]. These authors quantified both numbers and size (i.e., maximal diameter) of UBOs in three locations: hemispheres (e.g., globus pallidus), cerebellum (including deep cerebellar nuclei), and brainstem (including diencephalic structures). They found that while number and size of hemispheric and cerebellar UBOs decreased with age, those in the brainstem appear to increase [DiMario and Ramsby, 1998]. The discrepancy between these results, in particular those referring to the hemispheric lesions, and our data could be explained by several factors. While the

proportion of the sample with more than two observations is slightly larger in our analyses (58% vs. 47%), we postulate that our more comprehensive statistical analyses may have better recorded the changes over time in UBO parameters. An example of the strength of comprehensive longitudinal statistical approaches is the morphometric work conducted by Giedd and colleagues [1999]. These authors demonstrated cerebral gray matter volumetric increases throughout childhood (to a peak in adolescence), which have not been disclosed previously by cross-sectional analyses [Giedd et al., 1996; Reiss et al., 1996]. In support of our findings of non-linear evolution of lesions, other investigators have reported that T1-weighted signal hyperintensities associated with the typical UBOs [Mirowitz et al., 1989] tend to appear later in childhood and do not regress [Terada et al., 1996].

In addition to our more comprehensive statistical analytical strategy, the present study included a detailed anatomical parcellation. The latter separated related brain regions, which are distinct in terms of function or white matter structure (i.e., the most affected tissue component by UBOs). Despite this effort, we found, as did DiMario and Ramsby [1998], only two different regional patterns of evolution. One is characterized by decrease of lesions over time, which parallels the results reported by the two studies mentioned in preceding paragraphs, was the least common and was evident predominantly within the cerebellar hemispheres. Itoh et al. [1994] and DiMario and Ramsby [1998] also reported reductions of UBOs in the cerebellum; however, the latter authors did not differentiate medial structures such as the deep nuclei from the cerebellar hemispheres. In our data, medial cerebellar regions showed a mixed behavior; while the

number of lesions declined linearly with age, the volume of UBOs displayed a non-linear decrease-increase pattern. Another finding from our study, with relative agreement with the previous longitudinal study [DiMario and Ramsby, 1998], was the evolution of brainstem and diencephalic (mainly thalamic) lesions. The latter authors grouped both regions, which demonstrated an increase in UBOs over time. We also found an increase in lesions; however, this phenomenon was only seen during early adolescence.

The results presented here suggest that UBOs are a dynamic type of lesion, which not only develops during early childhood but also can appear during adolescence. The fact that of all locations only the cerebellar white matter shows a different evolution, with the previously reported decrease over time, may be a reflection of the unique nature of the UBO phenomenon. Whereas there is ample evidence that UBOs represent the "visible" manifestation of a more widespread process, as we demonstrated by MR spectroscopy (MRS) [Wang et al., 2000] and Steen and colleagues [2001] by T1 relaxometry, affecting predominantly the white matter [Itoh et al., 1994; DiPaolo et al., 1995; Yamanouchi et al., 1995; Said et al., 1996; Steen et al., 2001], the vast regions of cerebral hemispheric white matter are minimally involved [Itoh et al., 1994; Yamanouchi et al., 1995]. The exception seems to be the cerebellar white matter, which is frequently affected by the UBO process [Itoh et al., 1994]. We postulate that the distinctive distribution of UBOs, predominantly along major fiber bundles and centroencephalic regions [i.e., globus pallidus, thalamus] is linked to the compact packing of myelinated fibers in these locations [Carpenter, 1976]. Our recent diffusion tensor imaging (DTI) study of brainstem fiber bundles revealed that each major tract has a unique set of MR

parameters, including differences in MR T2 relaxation times [Stieltjes et al., 2001]. These MR properties may be in part responsible for the MRI features of UBOs. It appears that the less compact and more heterogeneous architecture of cerebral and cerebellar white matter make them less susceptible to develop long-term T2W hyperintense lesions. The fact that all three parameters evolved in a decrease-increase pattern, for most regions, suggests that initially developed multi-focal UBOs tend to regress in number and size and that the post-puberty increase simply represent an inverse process to the pre-teen involution. Whether the process corresponds to a "re-activation" of former lesions or the development of new UBOs is unclear, at this point, and deserves further examination.

The functional significance of UBOs is still a controversial issue. While there is evidence associating the presence of UBOs with many measured cognitive impairments [reviewed by North, 2000], the differential impact of lesion number and size is unclear. Denckla and colleagues [1996], using a model that predicts "lowering" of IQ relative to unaffected siblings, found that the number of UBO-occupied locations and not the proportion of tissue involved by UBOs or age was a significant predictive factor. In this regard our results, showing an increase in the number of affected locations during early adolescence, could help to re-evaluate the approach to lesion-deficit relationships in pediatric NF-1. In terms of association between UBO location and behavioral impairment, our findings do not provide additional insight. For instance, the reported correlation between thalamic UBOs and cognitive deficit [Moore et al., 1996] does not appear to be a reflection of a unique evolution of diencephalic UBOs.

In summary, this study on the longitudinal profile of T2W hyperintense lesions in children with NF-1 indicates that these lesions do regress during late childhood but reappear in early adolescence. Although this information is of great importance from the diagnostic viewpoint, taking into account the number of examined subjects, our investigation should be considered preliminary in nature. As in other quantitative neuroimaging studies [Giedd et al., 1999], we have taken advantage of the statistical power of longitudinal data, in which each sequential observation increases the strength of the data. Nonetheless, extension of the approach presented here to larger datasets will contribute to a more complete view of UBO evolution. Finally, integration of longitudinal UBO morphometry data with other quantitative neuroimaging methods, such as DTI, MRS, and T1 and T2 relaxometry, will ultimately lead to a better understanding of UBO pathophysiology and to specific therapeutic interventions.

ACKNOWLEDGMENTS

The authors thank Christine Koth for help in subject recruitment and Michael Abrams for assistance in data processing. This work was supported by grants P50 NS 35359 and P30 HD 24061 from the National Institutes of Health and an award from the US ARMY CDMRP.

REFERENCES

Aoki S, Barkovich AJ, Nishimura K, Kjos BO, Machida T, Cogen P, Edwards M, et al. 1989. Neurofibromatosis types 1 and 2: cranial MR findings. Radiology 172:527-534.

Brown EW, Riccardi VM, Mawad M, Handel S, Goldman A, Bryan RN. 1987. MR imaging of optic pathways in patients with neurofibromatosis. AJNR Am J Neuroradiol 8:1031-1036.

Carpenter MB. 1976. Human neuroanatomy. Baltimore: The Williams & Wilkins Co. 741 p.

Denckla MB, Hofman K, Mazzocco MM, Melhem E, Reiss AL, Bryan RN, Harris EL, et al. 1996. Relationship between T2-weighted hyperintensities (unidentified bright objects) and lower IQs in children with neurofibromatosis-1. Am J Med Genet 67 98-102.

DiMario FJJr, Ramsby G. 1998. Magnetic resonance imaging lesion analysis in neurofibromatosis type 1. Arch Neurol 55:500-505.

DiPaolo DP, Zimmerman RA, Rorke LB, Zackai EH, Bilaniuk LT, Yachnis AT. 1995. Neurofibromatosis type 1: pathologic substrate of high-signal-intensity foci in the brain. Radiology 195:721-724.

Giedd JN, Snell JW, Lange N, Rajapakse JC, Casey BJ, Kozuch PL, Vaituzis AC, et al. 1996. Quantitative magnetic resonance imaging of human brain development: ages 4-18. Cereb Cortex 6:551-560.

Giedd JN, Blumenthal J, Jeffries NO, Castellanos FX, Liu H, Zijdenbos A, Paus T, et al. 1999. Nat Neurosci 2:861-863.

Goldstein SM, Curless RG, Post MJD, Quencer RM. 1989. A new sign of neurofibromatosis on magnetic resonance imaging of children. Arch Neurol 46:1222-1224.

Gutmann DH, Aylsworth A, Carey JC, Korf B, Marks J, Pyeritz RE, Rubenstein A, et al. 1997. The diagnostic evaluation and multidisciplinary management of neurofibromatosis 1 and neurofibromatosis 2. JAMA 278:51-57.

Hurst RW, Newman SA, Cail WS. 1988. Multifocal intracranial MR abnormalities in neurofibromatosis. AJNR Am J Neuroradiol 9:293-296.

Itoh T, Magnaldi S, White RM, Denckla MB, Hofman K, Naidu S, Bryan RN. 1994. Neurofibromatosis type 1: the evolution of deep gray and white matter MR abnormalities. AJNR Am J Neuroradiol 15:1513-1539.

Mirowitz SA, Sartor K, Gado M. 1989. High-intensity basal ganglia lesions on T1-weighted MR images in neurofibromatosis. AJNR Am J Neuroradiol 10:1159-1163.

NIH. 1988. National Institutes of Health Consensus Development Conference: Neurofibromatosis Conference Statement. Arch Neurol 45:575-578.

North K. 2000. Neurofibromatosis type 1. Am J Med Genet 97:119-127.

Reiss AL, Abrams MT, Singer HS, Ross JL, Denckla MB. 1996. Brain development, gender and IQ in children. A volumetric imaging study. Brain 119:1763-1774.

Riccardi VM. 1999. Historical background and introduction. In: Friedman JM, Gutmann DH, MacCollin M, Riccardi VM, editors. Neurofibromatosis: phenotype, natural history, and pathogenesis. Baltimore: Johns Hopkins University Press. p 1-25.

Said SM, Yeh TL, Greenwood RS, Whitt JK, Tupler LA, Krishnan KR. 1996 MRI morphometric analysis and neuropsychological function in patients with neurofibromatosis. Neuroreport 7:1941-1944.

Steen RJ, Taylor JS, Langston JW, Glass GO, Brewer VR, Reddick WE, Mages R, Pivnick EK. 2001. Prospective evaluation of the brain in asymptomatic children with neurofibromatosis type 1: relationship of macrocephaly to T1 relaxation changes and structural brain abnormalities. AJNR Am J Neuroradiol 22:810-817.

Stieltjes B, Kaufmann WE, van Zijl PCM, Fredericksen K, Pearlson GD, Mori S. 2001. Diffusion tensor imaging and axonal tracking in the human brainstem. NeuroImage 14:723-735.

Terada H, Barkovich AJ, Edwards MS, Ciricillo SM. 1996. Evolution of high-intensity basal ganglia lesions on T1-weighted MR in neurofibromatosis type 1. AJNR Am J Neuroradiol 17:755-760.

Wang PY, Kaufmann WE, Koth CW, Denckla MB, Barker PB. 2000. Thalamic involvement in neurofibromatosis type 1: evaluation with proton magnetic resonance spectroscopic imaging. Ann Neurol 47:477-484.

Wechsler DL. 1974. The Wechsler Intelligence Scale for Children – Revised. San Antonio, TX: The Psychological Corporation.

Wechsler DL. 1991. The Wechsler Intelligence Scale for Children – III. San Antonio, TX: The Psychological Corporation.

Yamanouchi H, Kato T, Matsuda H, Takashima S, Sakuragawa N, Arima M. 1995. MRI in neurofibromatosis type I: using fluid-attenuated inversion recovery pulse sequences. Pediatr Neurol 12:286-290.

TABLE I. Anatomic Subdivisons For Lesion Localization

Region 1:	cerebral hemispheres (white matter)
Region 2:	corpus callosum
Region 3:	caudate
Region 4:	putamen
Region 5:	globus pallidus
Region 6:	claustrum/external capsule
Region 7:	internal capsule
Region 8:	thalamus
Region 9:	hypothalamus and subthalamus
Region 10:	(lateral) cerebellar hemispheres (white matter)
Region 11:	cerebellar vermis
Region 12:	deep cerebellar nuclei
Region 13:	dorsal midbrain
Region 14:	ventral midbrain (cerebral peduncles)
Region 15:	dorsal pons
Region 16:	ventral pons
Region 17:	middle cerebellar peduncle
Region 18:	medulla

A.

B.

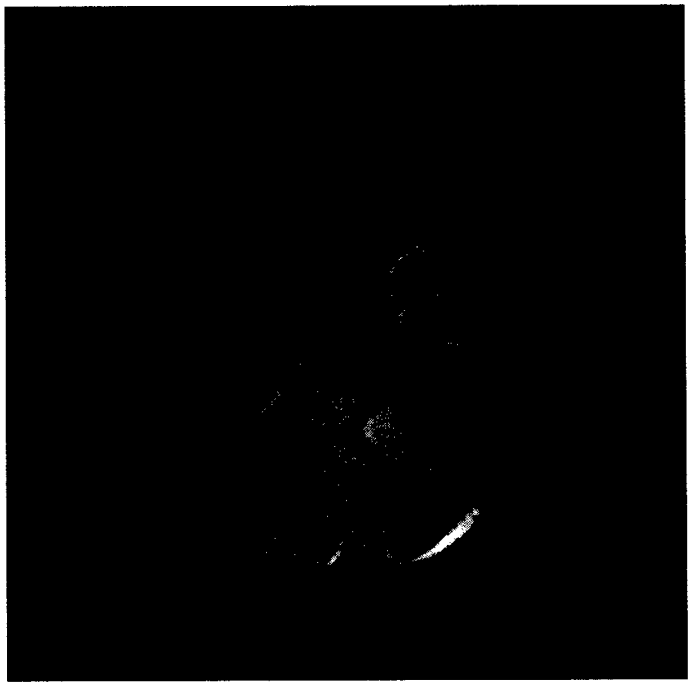

Figure 1. Proton density MRI scan showing UBOs on the right and left globus pallidus/internal capsule region. B. Same MRI sequence showing UBOs on both medial (left) and lateral (right) cerebellar regions.

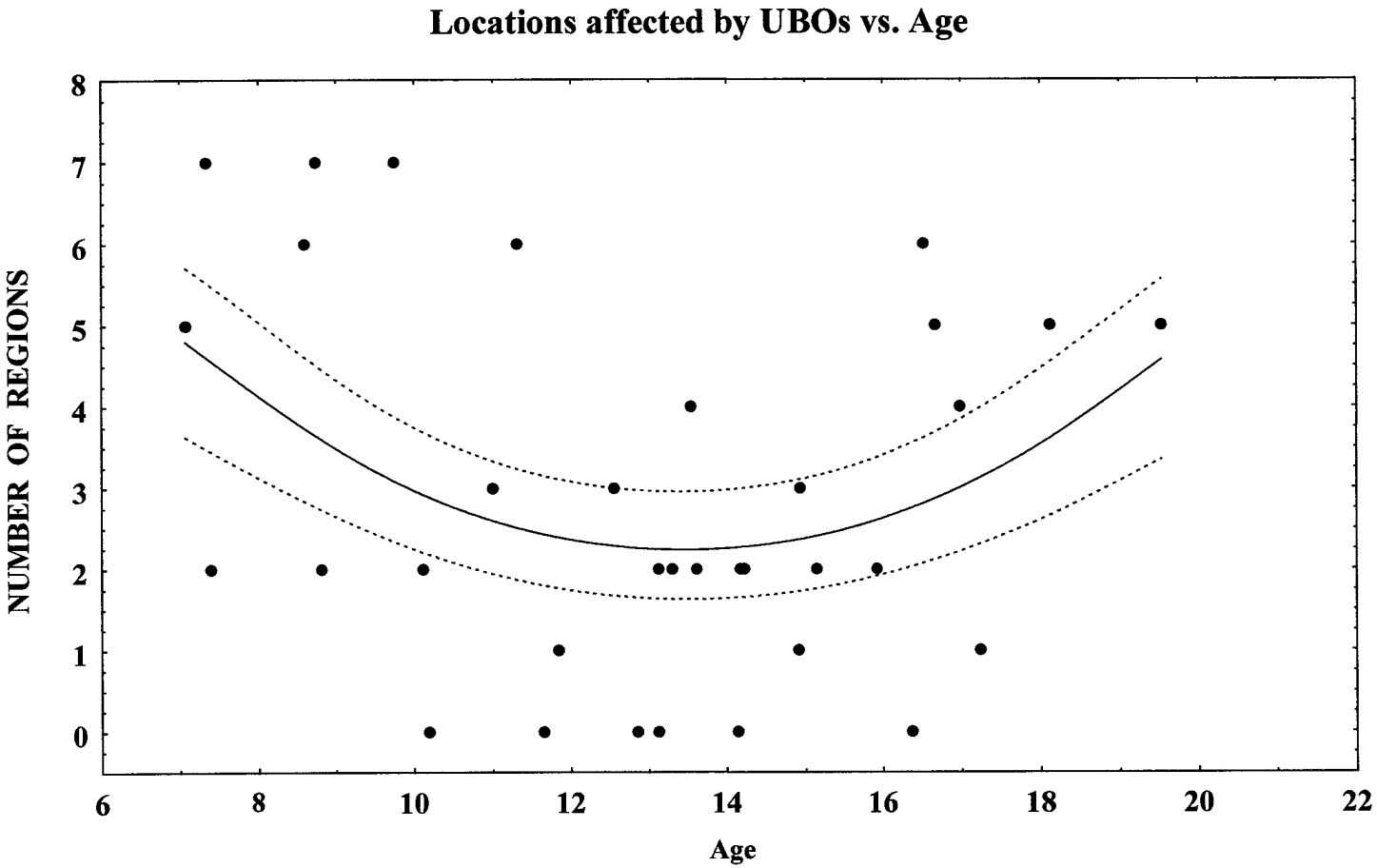

Figure 2. Number of UBO-occupied regions in function of age. Note the non-linear evolution of UBO distribution, with relatively high initial levels that decrease until 12-14 years of age, followed by a progressive increase during adolescence.

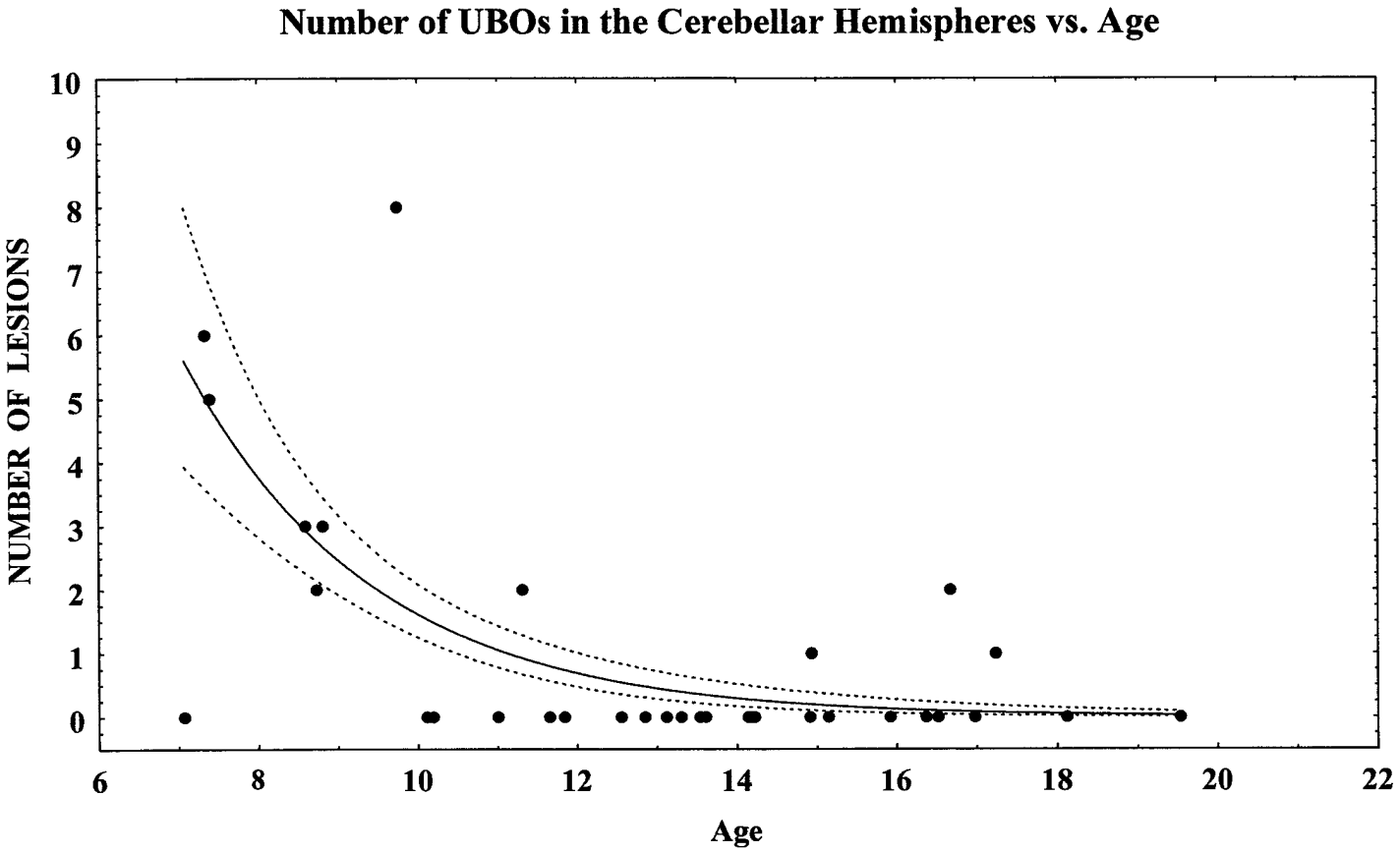

Figure 3. Number of UBOs in the cerebellar hemispheres (white matter) in function of age. Note the relatively linear evolution with steady decrease after high levels in early childhood.

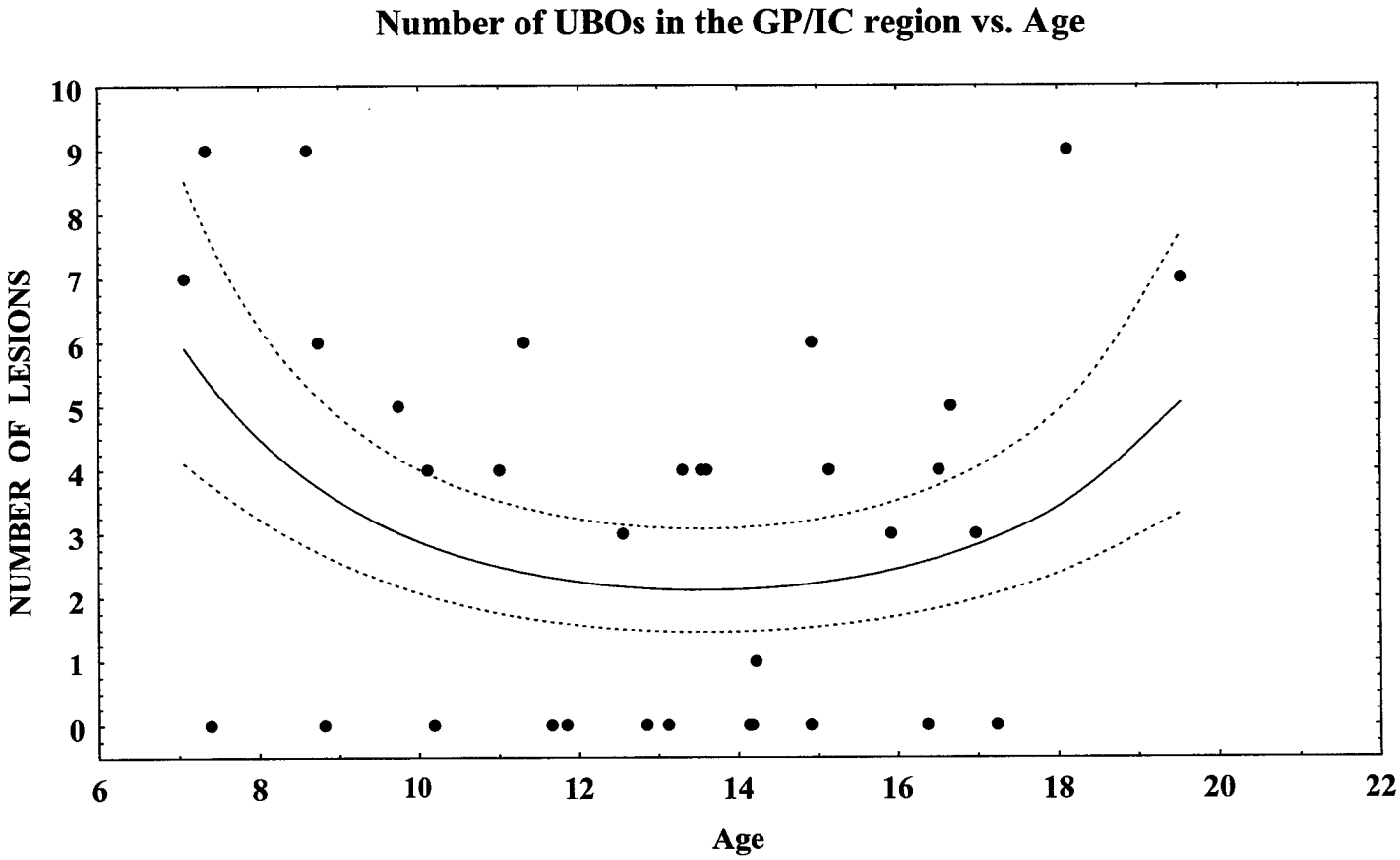

Figure 4. Number of UBOs in the globus pallidus/internal capsule (GP/IC) region in function of age. Note the non-linear evolution of UBOs with early decrease and late post-puberty increase, which resembles longitudinal pattern of UBO locations (see Fig. 2).

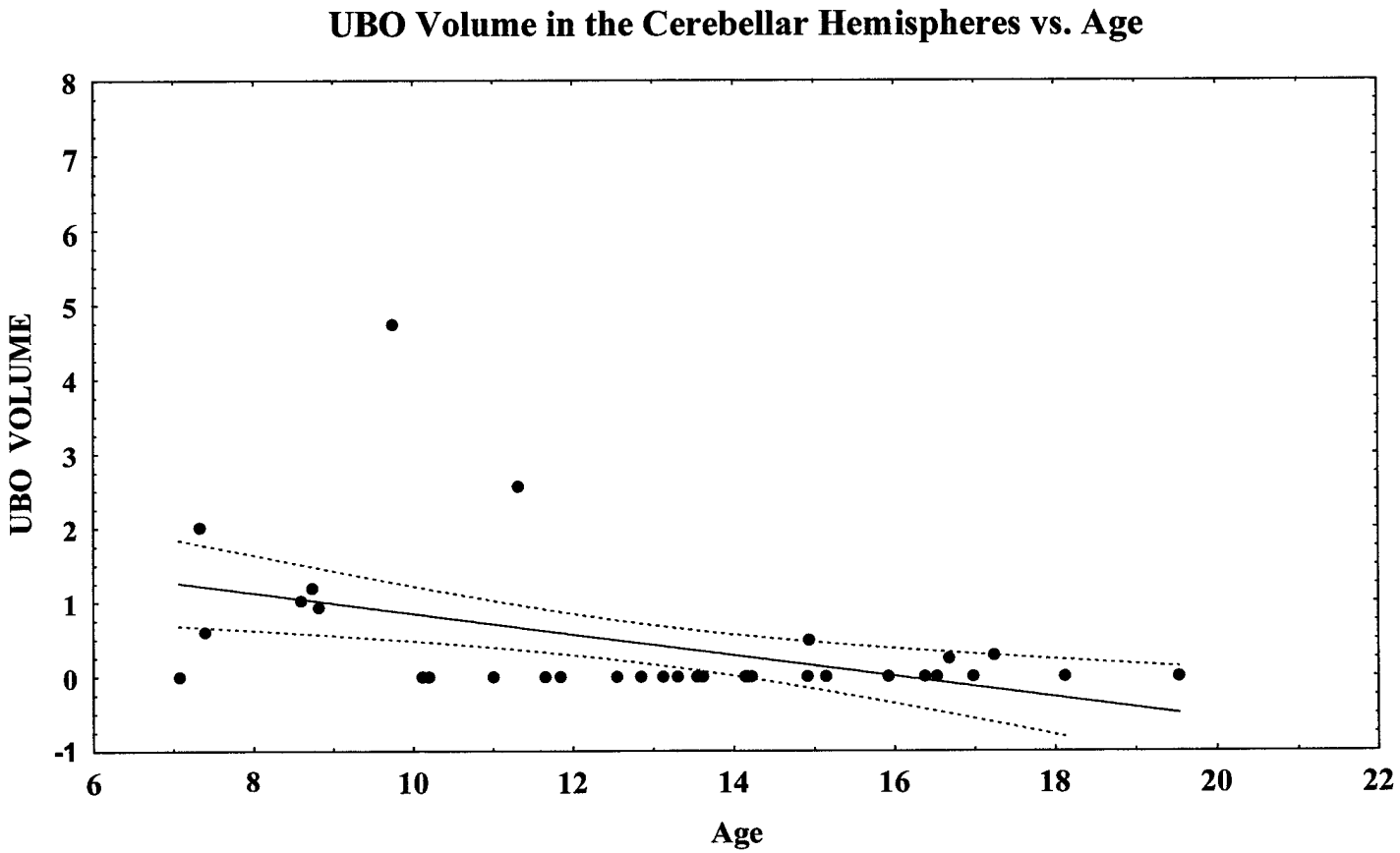

Figure 5. Volume of tissue (in cc) occupied by UBOs in the cerebellar hemispheres (white matter) in function of age. Note the linear decrease since early childhood.

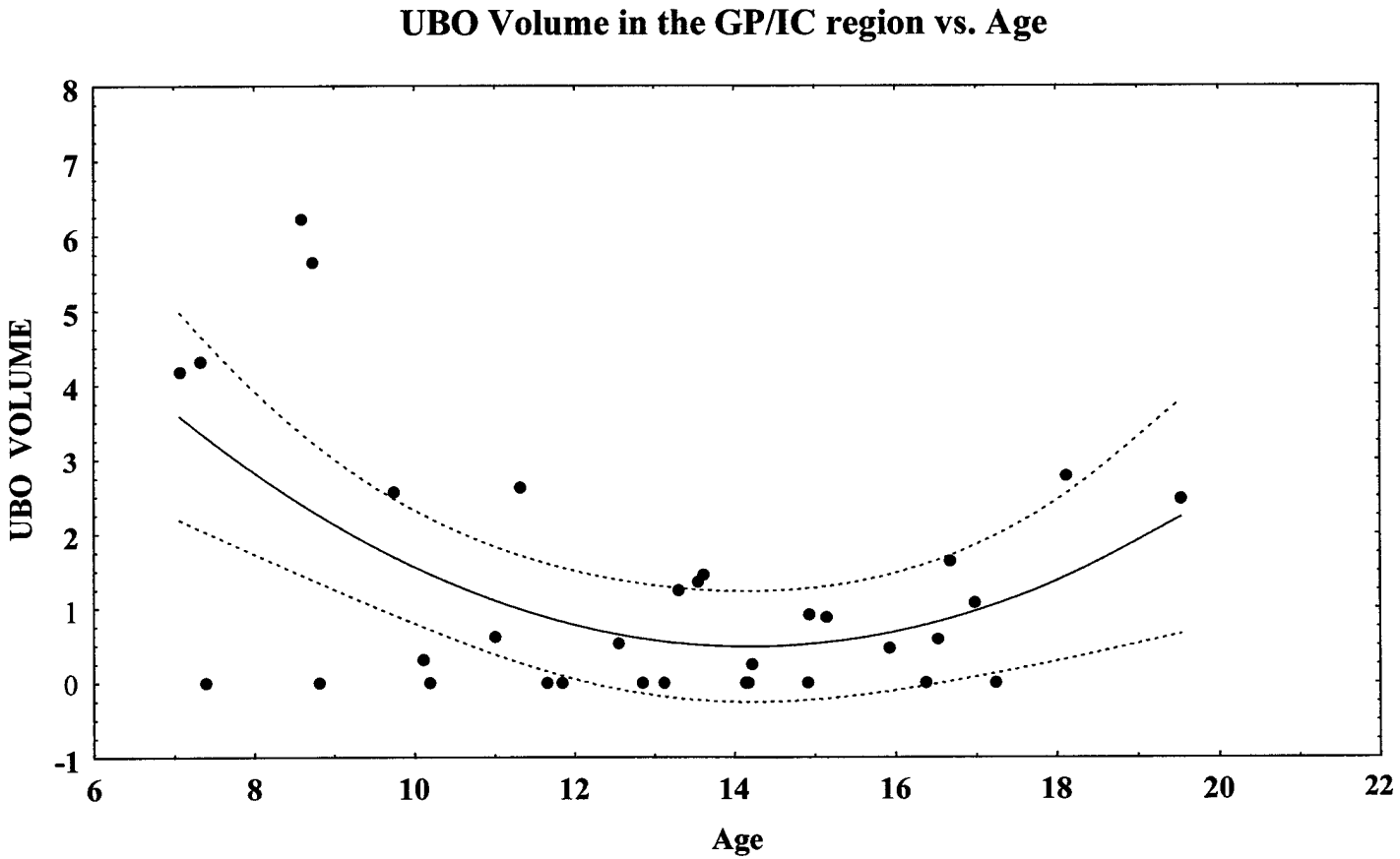

Figure 6. Volume of tissue (in cc) occupied by UBOs in the globus pallidus/internal capsule (GP/IC) region in function of age. Note the non-linear evolution of relatively large UBOs volumes in early childhood, which decrease to a minimum between 12-14 years of age, followed by a post-pubertal increase. A similar pattern of evolution can be seen in Figs. 2 and 4.